

# Aid Allocation for Camp-Based and Urban Refugees with Uncertain Demand and Replenishments

March 29, 2021

## Abstract

There are nearly 26 million refugees worldwide seeking safety from persecution, violence, conflict, and human rights violations. *Camp-based* refugees are those that seek shelter in refugee camps, whereas *urban* refugees inhabit nearby, surrounding populations. The systems that supply aid to refugee camps may suffer from ineffective distribution due to challenges in administration, demand uncertainty and volatility in funding. Aid allocation should be carried out in a manner that properly balances the need of ensuring sufficient aid for camp-based refugees, with the ability to share excess inventory, when available, with urban refugees that at times seek nearby camp-based aid. We develop an inventory management policy to govern a camp's sharing of aid with urban refugee populations in the midst of uncertainties related to camp-based and urban demands, and replenishment cycles due to funding issues. We use the policy to construct costs associated with: i) referring urban populations elsewhere, ii) depriving camp-based refugee populations, and iii) holding excess inventory in the refugee camp system. We then seek to allocate aid in a manner that minimizes the expected overall cost to the system. We propose two approaches to solve the resulting optimization problem, and conduct computational experiments on a real-world case study as well as on synthetic data. Our results are complemented by an extensive simulation study that reveals broad support for our optimal thresholds and allocations to generalize across varied key parameters and distributions. We conclude by presenting related discussions that reveal key managerial insights into humanitarian aid allocation under uncertainty.

**Keywords:** Inventory Management, Humanitarian Aid, Nonlinear Optimization, Stochastic Modeling.

# 1 Introduction

As of June 2019, the United Nations High Commissioner for Refugees (UNHCR) estimated that well over one-third of the 70.8 million forcibly displaced people worldwide, nearly 26 million, are *refugees*: displaced peoples that have both crossed an international border in search of safety, and have been granted corresponding status (UNHCR, 2019). The number of refugees and displaced peoples continues to rise over the last decade due to increasing conflicts, famines, and natural disasters. When compared with just ten years earlier (UNHCR, 2009), this most recent 2019 figure represents a staggering 70.4% increase (UNHCR, 2019).

The refugee crisis is global in scope, not limited by regional or continental borders. Over a quarter of the 25.9 million global refugees, around 6.7 million, are as a result of the ongoing conflict in Syria that emerged in 2011. Beyond Syria, additional hot spots of origin include Afghanistan (2.7M), South Sudan (2.3M), Myanmar (1.1M), and Somalia (0.9M). Countries hosting significant refugee populations include Turkey (3.7M), Pakistan (1.4M), Uganda (1.2M), Sudan (1.1M), and Germany (1.1M). Per capita, Lebanon leads the way, where 1 in 6 persons are refugees, followed by Jordan (1 in 14) and Turkey (1 in 22) (UNHCR, 2019).

*Camp-based* refugees seek shelter in refugee camps, whereas *urban* refugees seek support in nearby populations (UNHCR, 2019). Whether a refugee is seeking support while living inside of (*internal* to) camps, or while living in surrounding urban areas (*external* to camps), each type faces their own particular circumstances<sup>1</sup>. Urban refugees have somewhat improved mobility and better vocational prospects, and yet may be at greater risk of exploitation (UNHCR, 2019). The alternative is not much easier for camp-based refugees. Although there is a degree of stability that comes with camp life, the living conditions are hardly enriching, they are closer to subsistence (UNHCR, 2016), and can engender dependency (UNHCR, 2014).

Camp life poses a number of significant challenges. Camp-based refugees are particularly susceptible to outbreaks of vaccine-preventable diseases<sup>2</sup> due to compromised health and nutrition states, and less than desirable sanitation conditions (Lam et al., 2015). Moreover, overcrowding is commonplace, owing to surges in refugee populations from ongoing conflicts and persecution<sup>3</sup>. These influxes affect camp-based and urban refugee populations alike, causing sharp increases in the need for humanitarian aid like food, clothing, and medicine. Even for stable camp populations, the level of available supplies may be insufficient to meet fluctuating demand between aid replenishment cycles; the needs of nearby urban refugees only intensify these shortages.

Beyond the uncertainty in demand for humanitarian aid among refugee populations, agencies responsible for providing assistance often face supply shortages (UNHCR, 2015), in particular during the emergency and post-emergency phases (IOM, NRC, and UNHCR, 2015). Distribution, including regular replenishment, suffers from a lack of structured planning and coordination and volatility in funding cycles (IOM, NRC, and UNHCR, 2015; Simmons, 2016; Dunn, 2016; Altay and Narayanan, 2020), leading to uncertain downstream access to essential aid (Terefe, 2017; Al-Rousan et al., 2018). Indeed, uncertainties in demand, as well as distribution and inventory

---

<sup>1</sup>As per UNHCR (2019), we categorize refugees as *camp-based*, or *urban*. Where unambiguous and convenient, we also use *internal* to indicate *camp-based* refugees, and both *external* and *surrounding* to signify *urban* refugees.

<sup>2</sup>Indeed, at the time of this writing, the deadly coronavirus outbreak threatens to ravage camp-based refugee populations, like on the island of Lesbos (Fallon, 2020). Elsewhere, in response to the pandemic, all 39 Rohingya refugee camps in Cox’s Bazar, Bangladesh have suspended every non-essential activity (Solomon, 2020).

<sup>3</sup>Ongoing political instability in Venezuela led to more than 340,000 new asylum applications in 2018 (UNHCR, 2019). Bangladesh and several other countries in Southeast Asia have absorbed waves of fleeing Rohingya refugees; in late 2017, nearly 700,000 Rohingya refugees fled the Rakhine state of Myanmar due to ethnic cleansing and genocide (UNHCR, 2019). As a result of the ongoing civil conflict in Syria, Tumen (2016) studied the “exogenous immigration shocks” and resulting impacts on the market in Turkey.

management, underscore the difficulty in accurate estimation of humanitarian aid availability in refugee camps (Terefe, 2017). Such uncertainties must be properly addressed in the design and operation of humanitarian supply chains (Jahre et al., 2016).

Aid agencies are primarily charged with serving camp-based refugee populations. That said, they may also serve a portion of urban demand when resources allow. A recent survey of Syrian refugees in Turkey suggests that aid distribution can be experienced as unfair, placing both camp-based and urban populations at risk of adverse health effects (Al-Rousan et al., 2018). This leads to two critical questions concerning the equitable distribution of critical aid to refugees amid uncertainty in camp-based and urban demand, as well as time until replenishment: *How should humanitarian aid be distributed from a central decision-maker to a refugee camp system? And, at what point should a camp reserve aid for camp-based refugees, rather than sharing with nearby urban refugee populations?*

If sufficient supplies are expected, it may be beneficial to share resources with nearby urban refugees. However, this must be balanced: if aid is given to an external request, future internal (and external) demands may suffer from eventual shortages, given the variable nature of replenishment cycles. We consider three costs to characterize these tradeoffs: that of referral, when an external (urban) request for aid is denied; that of deprivation, when an internal (camp-based) request for aid is unable to be satisfied (Holguín-Veras et al., 2013); and that of holding excess inventory. These components underscore the inherent tradeoffs of aid sharing in resource-scarce refugee camp systems, where excess supply and demand depends on replenishment cycles, which are uncertain. Given the limited resources, accurate decisions are critical.

We make the following contributions. First, in light of uncertainties in medical aid distribution, namely camp-based demand, urban demand, and replenishment cycle duration, we a) present a stylized inventory management system and b) derive a sharing threshold (decision rule) for each refugee camp, below which the expected cost of satisfying a demand occurrence from urban refugees causes a higher expected cost than rejecting that request and referring elsewhere. Second, we use these thresholds to define piecewise functions for expected referral, deprivation, and holding costs, respectively; in so doing, we contribute to the steadily growing literature that explicitly incorporate the concept of deprivation into cost expressions (Holguín-Veras et al., 2013), which enables our model to capture the impact of suffering with respect to delays in aid demand satisfaction within a long-term relief distribution setting. Summing these individual costs yields an expected total cost function for each camp. Third, we obtain the expected total cost for the entire camp system by summing the individual expected total cost functions over each camp, which we then embed in a cost-minimizing nonlinear optimization model. This model seeks to optimize the quantities of aid to be allocated from a central decision-maker to each refugee camp at the beginning of a replenishment cycle, to primarily emphasize service for residents of the camp, while secondarily providing assistance to refugees living outside of camps with potentially excess inventory. In other words, under uncertainty in demand and cycle duration, we model the optimal allocation of aid and associated interaction between the service of primary and secondary sources at each camp location when the two sources consume homogeneous inventory of a single type. Fourth, we develop two solution methods: an analytical approach where for each camp it is a priori known whether the aid allocation level exceeds the threshold, and a more general approach that uses a piecewise linear representation of the nonlinear objective function. We use the latter approach to study aid allocation for a Syrian refugee camp system in southern Turkey motivated by real data, as well as for synthetic datasets. Fifth, we validate our results by an extensive simulation study that shows broad support for our optimal thresholds and allocations to generalize across varied key parameters and distributions. Finally, we analyze

the obtained results and conclude by offering insights on managing humanitarian aid in refugee camp settings.

The remainder of this paper is organized as follows. In § 2 we survey the literature on humanitarian (and in particular refugee) operations, focusing on operations research and inventory models. In § 3 we formally define our problem, and in § 4 we derive our camp inventory management policy at both the micro (inventory control) level and macro (allocation) levels, and present an optimization formulation to address the optimal allocation of aid under derived sharing thresholds along with two solution approaches. In § 5 we conduct computational experiments to assess the performance of our mathematical models, and discuss managerial insights from both a case study in the context of Syrian refugee camps in southern Turkey, as well as synthetic datasets. Finally, we provide concluding remarks, limitations, and directions for future research in § 6.

## 2 Literature Review

Refugee crises fall under the category of *complex* emergencies in the literature, and can be viewed according to their phase. The emergency phase represents the onset of displacement, where life-saving efforts is the primary focus. Greater stability marks the post-emergency phase, where the emphasis shifts from meeting basic needs, to providing sustainable solutions, and may be prolonged in nature. The third and final phase coincides with the identification of durable solutions, and camp inhabitants may leave the camp (IOM, NRC, and UNHCR, 2015; UNHCR, 2018).

Unlike natural disaster relief efforts that typically last for less than one year, aid operations for refugees may continue for a number of years due to the displacement and resettlement of unexpected foreigners into host countries (Balcik et al., 2016). Moreover, the responses frequently extend beyond the capabilities of a single humanitarian agency, and aid distribution often takes place in an ad hoc manner across multiple agencies (UNICEF, 2007; Beamon and Kotleba, 2006a; Dunn, 2016). There are various sources of uncertainties in managing these humanitarian crises. These include variability of cycle duration for aid products due to the availability of aid agency funding (Brookland, 2012), availability of accurate supply information (Swaminathan, 2010), and uncertainties in refugee demand for aid in terms of timing and location (Beamon and Kotleba, 2006b).

The use of analytical approaches to address migration and refugee challenges is a relatively new area of study in humanitarian operations. Karsu et al. (2019) provide a review of the processes related to refugee camp management from an operations research perspective, categorizing refugee camp management into establishment and administration phases. They address challenges faced in refugee camps and propose analytical approaches for each. Other studies introduce a variety of models to address refugee challenges, such as camp (facility) location, relief distribution, and matching in refugee resettlement. Vatasoiu et al. (2015) develop a multi-objective mixed-integer program to optimally choose the locations and sizes of short-term refugee camps in Syria; the goal is to minimize total cost including startup and maintenance cost, while ensuring camp safety and reachability for refugees and aid workers. Buluç (2018) investigates the distribution of cash and e-vouchers to refugees and routing of trucks providing Child Friendly Spaces to vulnerable refugee children; covering vehicle routing problems, as well as heuristics, are proposed, and their performance evaluated on real data from Kilis, Turkey. Ahani et al. (2021) as well as Bansak et al. (2018) consider refugee resettlement, using machine learning and optimization to assign refugees to initial locations for the purpose of improving integration outcomes for both refugee and destinations. Ahani et al. (2021) additionally introduce the *Annie*<sup>TM</sup> MOORE software plat-

form that enables interactive visualization and re-optimization of the match outcome decision space.

The inventory management literature in humanitarian settings can be categorized according to the disaster management cycle they address: disaster *preparedness*, and disaster *response* (Balcik et al., 2016). Disaster preparedness studies typically focus on long-term, pre-disaster decisions around the locations and amounts of pre-positioned goods. On the other hand, disaster response efforts tend to focus on managing relief inventory in the post-disaster setting, so as to ensure that needed demand is satisfied in the most efficient way. While a number of interesting studies exist of the former type, we focus on the latter which is more pertinent to our study.

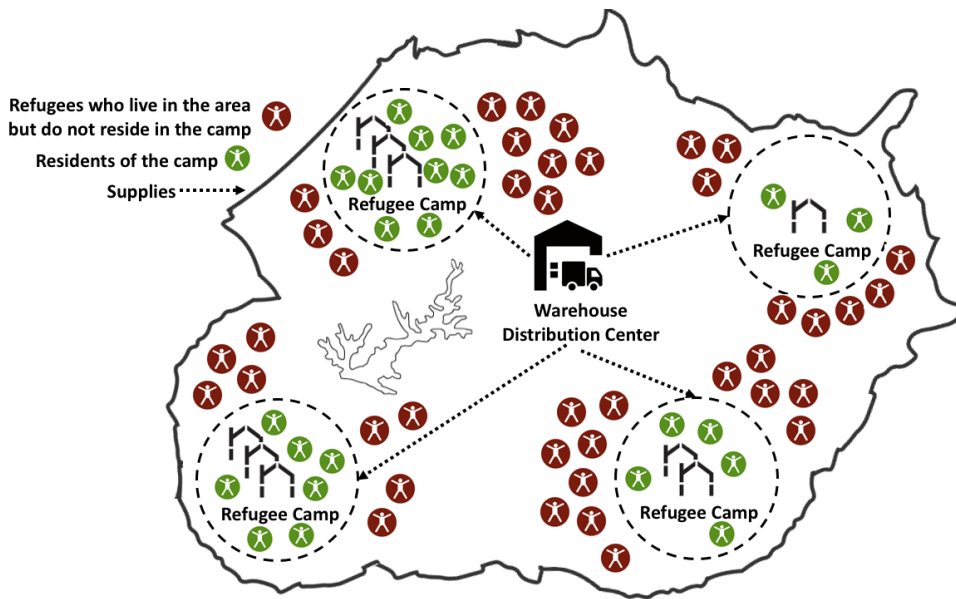
Beamon and Kotleba (2006b) propose a  $(Q, R)$  model with regular and emergency orders for long-term humanitarian operations, where emergency orders are only placed due to a sudden increase in demand, and backorders are allowed. They provide an analytical solution for refugee operations due to the civil war in South Sudan; a Silver-Meal heuristic for this problem is introduced in Beamon and Kotleba (2006a). McCoy and Brandeau (2011) also develop a  $(Q, R)$  model with regular and emergency orders, in which they consider the decision on proportions of budget allocated to shipping and stockpiling. Natarajan and Swaminathan (2014) consider a problem setting where total amount of funding during a time horizon is known, but exact amounts of funding in each time period is uncertain, in addition to uncertainties in demand occurrences. Under these uncertainties, they propose a periodic review inventory policy which aims to minimize expected total holding, backordering, and ordering costs. Natarajan and Swaminathan (2017) extend this study by including multiple states for the applied treatment.

A hallmark of modeling inventory-related operations in humanitarian logistics is the development of objective functions that embody notions beyond traditional financial measures. That is, additional altruistic characteristics are often considered, such as maximizing the amount of demand satisfied or minimizing the lead time (see, e.g., Balcik and Beamon, 2008; Mete and Zabinsky, 2010; Salmerón and Apte, 2010; Duran et al., 2011; Rennemo et al., 2014). To ensure demand coverage is maximized, some studies associate a penalty cost with unmet demand and seek its minimization (Rawls and Turnquist, 2010). Another stream of research focuses not only on modeling responsiveness and timely demand satisfaction, but also include a penalty for unmet demand in terms of *deprivation* cost, thereby representing human suffering from unmet need (Holguín-Veras et al., 2013). As the timeliness of demand satisfaction for camp-based refugees is of first-order importance, we model any shortages as deprivation costs; secondarily, we model the timeliness of demand satisfaction in the surrounding population as referral costs. Our study is situated among post-disaster inventory management models for complex emergencies. We consider aid administration and distribution in refugee camp systems, deriving and proposing a centralized inventory management policy for existing refugee camps. To the best of our knowledge, no study has simultaneously considered inventory allocation and management in refugee operations from the perspective of a centralized decision-maker, while measuring timeliness of demand satisfaction, and taking into account uncertainties in camp-based and urban demand occurrences and replenishment cycles. While a number of studies include one or more of these aspects so commonly faced by humanitarian agencies separately, we believe we are the first to consider them in a single model. This enables us to propose an inventory policy that can be used to improve the efficiency in refugee operations management, resulting in both greater numbers of refugees served, as well as reduced inventory and deprivation.

### 3 Problem Definition

Modalities to address protracted refugee crises around the world include the more traditional refugee camp solutions featuring centralized, top-down, one-way flows of aid, as well as newer initiatives that acknowledge the inherent human desire for agency and independence, and feature localized service options and two-way flows of resources (Landau, 2014; Jahre et al., 2018). In light of the prevalence and established structure of the former (UNHCR, 2014; Jahre et al., 2018), we consider a central decision-maker<sup>4</sup> that distributes medical aid<sup>5</sup> via a single warehouse distribution center to an existing refugee camp system, that is, an arrangement of refugee camps. This is illustrated in Figure 1, where a centralized distribution center allocates supplies to individual camps within the refugee camp system.

Figure 1: Refugee Camp System Illustration, with Central Distribution to Multiple Refugee Camps. Both Camp-Based and Urban Refugee Populations are Depicted.



Each camp is responsible for internal, camp-based refugees, while potentially serving urban refugees that live in communities external to the camp, but within a reachable distance. For urban refugees, receiving in-camp care has both advantages and disadvantages. Whereas refugees are more likely to be satisfied with the quality of urban healthcare systems (Crea et al., 2015), they may face language challenges and a general lack of knowledge on how the host country healthcare system operates (Torun et al., 2018). At the same time, access to camp-based healthcare is easier, less costly, and has less cultural barriers (Dorai, 2010). In Palestine and Jordan, for instance, urban refugees often visit camp healthcare services because they are less costly and well-connected to the surrounding villages (Dorai, 2010; Howayek, 2015). In light of the presence of urban refugee demand, camp inventory must therefore be properly managed.

Thus, while the priority is to serve camp-based refugees, nearby urban refugees requesting aid may be assisted if sufficient inventory exists. If the request is denied, then the unit of aid is maintained in camp inventory, but the system incurs a cost of referring that refugee elsewhere

<sup>4</sup>This may be any organization coordinating aid distribution, such as the UNHCR, a national government, or other aid agencies.

<sup>5</sup>Our focus is on medical supplies, specifically routine medicine such as painkillers and first aid kits, as well as certain elective vaccines (such as influenza and HPV).

for care, such as to a hospital in the surrounding area. Hence, external requests should be accommodated where it is expected that sufficient inventory exists. However, once the camp inventory is exhausted, neither external nor internal future requests can be satisfied until the next replenishment from the single centralized supplier, generating both referrals for external populations and deprivation for internal populations.

In the emergency and post-emergency phases of refugee crises, camps initially lack even basic health services, gradually stabilizing with respect to staffing, material resources, support systems, security, funding, and coordination (IOM, NRC, and UNHCR, 2015). The nature of the environment leads to a general absence of organized stock policies and the use of heuristics for stocking decisions, resulting in inefficient inventory management practices (McCoy and Brandeau, 2011; Dunn, 2016). Throughout the emergency and post-emergency stages, timing between replenishments of aid products can vary widely due to multiple factors, such as availability of funding for aid agencies, accessibility of required products from agreed-upon suppliers, and supply chain mismanagement (Mizushima et al., 2008; Swaminathan, 2010; Brookland, 2012; Natarajan and Swaminathan, 2014, 2017). This funding volatility and mismanagement creates uncertainty around the amount of time elapsed since the last replenishment, suggesting a memoryless replenishment distribution. Similar to that of Natarajan and Swaminathan (2014), for the replenishment cycle length we also adopt an exponential distribution on independently and uniformly distributed installments within each funding cycle, as it has been shown that occurrences of events with exponential interarrival times in a given time interval are distributed independently and uniformly (Ross, 2014).

Refugee demands for critical aid such as medicine are uncertain (Beamon and Kotleba, 2006b). Many real arrival and demand processes, including emergency services such as police, fire and ambulance, have been empirically shown to be very well approximated by a Poisson process; in healthcare, considering the size of the population, the Poisson process has been verified to be a good representation of unscheduled arrivals to various parts of hospitals (Kim et al., 1999; Green et al., 2006; Green, 2006). Hence, as the number of refugees requiring assistance is large, and each requires assistance with low probability, we model the demand uncertainty via Poisson-distributed occurrences for both camp-based refugees and urban refugees at each refugee camp.

We consider long-term relief cycles for refugee aid from a centralized decision-maker perspective, such as those in regions suffering prolonged humanitarian crises, where lack of aid may exacerbate suffering, and hence the need to consider associated costs that follow. In an effort to value human suffering, we develop a deprivation function that represents the nonlinearly increasing effect of prolonged need for medical supplies affecting the quality of life of camp-based refugees. We incorporate deprivation costs into our model alongside the traditional logistics costs of holding and referral, as the level of service and timeliness of demand satisfaction is of vital importance for the population in need (Holguín-Veras et al., 2013). Although it necessarily adds complexity, this approach represents a broader and more realistic problem setting.

The system seeks to serve the greatest (weighted) number of refugees, with demand from camp-based refugees necessarily having a higher priority than that of urban refugees. Thus, there are two issues that require further investigation related to the dynamics of this refugee camp allocation system. First, a rule for each camp must be established to ensure that priority is given to camp-based refugees in terms of aid demand. Moreover, due to the stochastic nature of replenishments, the quantity allocated to each of the camps should be determined considering the trade-off between camp-based and urban populations, as well as their associated arrival rates and incurred costs.

We develop a mathematical approach that focuses on the trade-off between satisfying the needs of both camp-based and urban refugees, while respecting available resources. We accomplish

this via an optimization model in which a central decision-maker decides on the quantities to be allocated to each camp by minimizing the expected total cost of the system per replenishment cycle, in the presence of a limited supply to distribute. Let  $\mathbf{X} = [X_1, \dots, X_i, \dots, X_N]$  be an integer-valued vector that represents the *order up to* level of a single type of aid commodity to be allocated to each camp  $i$  in the system.

**Remark 1.** *As the order up to level defines the allocation decisions to camps in conjunction with existing inventory and expected duration until the next replenishment, the decisions we consider can alternatively be thought of as allocation decisions. Thus, where unambiguous, we also use allocation to refer to the vector  $\mathbf{X}$ .*

The expected total cost function to be minimized,  $E[C^T(\mathbf{X})]$ , is composed of several separate cost components including referral, deprivation, and holding. To maintain consistency, we allow for a slight abuse of notation, using  $C^T(X_i)$  to denote the total costs for allocation to a single camp  $X_i$ , and  $C^T(\mathbf{X})$  for the same over the entire camp system allocation.

**Referral cost.** This component is the cost of referring a request for aid from an urban refugee elsewhere for care, such as a hospital system in the nearby area. It assesses the trade-off cost between keeping inventory for future demand occurrences within the camp, and fulfilling the aid request from the surrounding population of the camp. Expected referral costs are calculated in § A.3.1.

**Deprivation cost.** This component is the cost of unfulfilled demand from camp-based refugees. Because the priority of each camp is to satisfy internal demand, the needs of the surrounding, urban populations naturally play a lesser role. Therefore, the inability to satisfy an internal aid request incurs a cost for the camp system that increases in a nonlinear manner over time until the next replenishment arrives. Expected deprivation costs are calculated in § A.1 and § A.3.2.

**Holding cost.** This component is the cost related to keeping inventory in the system, the consideration of which compels the system toward lower amounts of inventory. Expected holding costs are calculated in § A.3.3.

Our methods provide a means to allocate a single type of scarce aid commodity to multiple camps within a refugee camp system in a manner than minimizes expected total cost. The optimal allocation prescribes a target level of replenishment for each camp, while giving preference to serve camp-based refugees.

## 4 Mathematical Developments

This section presents the mathematical modeling we develop to address the allocation of aid to individual refugee camps within a centralized refugee camp system when considering uncertainties in replenishment cycle duration, as well as internal and external demand. First, for each camp in the system we establish a decision rule, or threshold, for sharing inventory with the surrounding refugee population. Second, according to these thresholds we develop piecewise functions to represent costs of referral, deprivation, and holding, which when summed represent the expected total cost per camp. Third, we develop a nonlinear optimization model that seeks to minimize the expected total cost over all camps by optimizing aid allocation decisions. Fourth, we provide two solution approaches. The first handles the special case that assumes a priori knowledge of the inventory levels with respect to the derived sharing thresholds, and leverages KKT conditions to derive to optimal inventory levels. The second solves the more general problem of determining optimal aid allocation levels without foreknowledge of its relationship with sharing thresholds. It does so by employing a piecewise linear approximation of

the nonlinear (expected) total cost function. This latter approach enables model tractability while guaranteeing global optimality within any desired degree of accuracy. We provide open source code for our solution methods to make available to stakeholders involved in similar aid allocation problems.

#### 4.1 Formal Problem Setup

We consider a centrally managed refugee camp system comprised of multiple camps, where there is relative scarcity in the aid resources to be allocated at each cycle. We assume the priority of the centralized decision-maker is the timely satisfaction of aid requests for refugees living within camps, with a secondary consideration for the satisfaction, when possible, of aid requests from refugees living outside of camps. Because priority is given to internal demand satisfaction for each camp, we assume no separate inventory exists for refugees in the respective neighboring populations. Rather, we consider external demand occurrences at each camp as separate systems with *base-stock* inventory levels of zero, and reactively replenished from the internal camp inventory by a single unit of aid to fulfill the external demand request. Table 4 contains the nomenclature we use in our mathematical developments.

Table 4: Nomenclature.

Notation	Description
$N$	Number of camps in the camp system, where camps are indexed by $i$
$\lambda_i^C$	Rate for Poisson distributed internal (camp-based) demand for aid at camp $i$
$\lambda_i^U$	Rate for Poisson distributed external (urban) demand for aid at camp $i$
$\mu$	Rate for exponentially distributed time between replenishment cycles
$\delta_D$	Deprivation coefficient
$\alpha$	Deprivation rate
$D(T)$	Deprivation cost of unmet internal demand of duration $T$
$\delta_R$	Referral cost for unmet external demand
$h$	Holding cost per time unit
$I_i$	Initial inventory at each camp $i$
$\mathbf{I}$	Vector of initial inventories over all camps in system
$X_i$	<i>Order up to</i> level of inventory allocated by central decision-maker for each camp $i$
$\mathbf{X}$	Vector of <i>order up to</i> levels over all camps in system
$\Omega_i$	Threshold for sharing aid with external urban populations at camp $i$
$C^T(\cdot)$	Total cost of allocation $X_i$ (camp) or $\mathbf{X}$ (system)
$S$	Allocable supply from central decision-maker to camps in system

When an urban refugee requests one unit of aid from a camp, the request can either be accepted and the demand is satisfied with no cost, or the refugee is referred for care elsewhere, and a referral cost,  $\delta_R$ , is incurred. However, if the demand of a camp-based refugee goes unsatisfied due to depletion of all inventory prior to the duration of the replenishment cycle, the system incurs deprivation cost  $D(T)$  for that demand occurrence for the amount of time  $T$  that the internal demand is left unfulfilled. Thus, if the unit of aid is provided to a refugee from the surrounding population and the camp inventory becomes zero prior to the end of the current cycle, the system will incur a penalty cost that increases in a nonlinear manner over time until replenishment arrives, for any excess demand that is observed. Hence, the system would incur

a higher cost due to the additional deprivation costs. In contrast, if the request of an urban refugee goes unfulfilled and yet there is remaining inventory at the end of the replenishment cycle, a system state must exist with strictly less cost. Therefore, a clearly defined decision rule for sharing is needed for the system to operate in a more efficient manner. We propose an inventory model that prioritizes internal demand occurrences by explicitly defining for each camp a sharing threshold, above which urban refugee demands are satisfied by their respective camps, and below which such refugees are referred elsewhere with an associated cost.

## 4.2 Inventory Control Policy and Related Cost Derivations

The aid inventory control policy for a camp depends upon a certain threshold. When the aid inventory level exceeds this threshold, the policy is to fulfill both internal and external demand; otherwise, aid should be designated for internal demand only, thereby rejecting external demand. Therefore, the trade-off when sharing inventory with external populations is between referring urban refugees, and deprivation for *unfulfilled camp-based demand*. We first formalize our inventory control policy.

**Definition of Sharing Threshold.** *When the inventory level is above the sharing threshold, the camp fulfills both internal (camp-based) and external (urban) demand. Otherwise, the camp only fulfills aid for internal demand, referring external demand elsewhere in the surrounding area.*

To explicitly derive the sharing threshold, we now express the deprivation cost for a single internal refugee.

**Lemma 1.** *If the inventory reaches zero and a unit of aid is demanded internally, the expected deprivation cost for this arrival until the next replenishment is:*

$$E[D(T)] = \frac{\delta_D \alpha}{\mu - \alpha} \text{ for } \alpha < \mu. \quad (1)$$

*Proof.* The proof appears in Appendix A.1. □

Equation (1) shows that if  $\delta_R \geq \frac{\delta_D \alpha}{\mu - \alpha}$ , then even with a single unit of aid in stock, referring an urban refugee request elsewhere would incur a higher penalty, which implies a policy of always sharing. Therefore, we make the following remark.

**Remark 2.** *To ensure that sharing is at some point undesirable and thus have a positive sharing threshold, we make the assumption that  $\delta_R < \frac{\delta_D \alpha}{\mu - \alpha}$  holds.*

We now present the central result in our study, Theorem 1, which address the micro-level problem by expressing the sharing threshold for each camp  $i$ .

**Theorem 1.** *The threshold above which camp  $i$  should share aid inventory is:*

$$\Omega_i = \left\lceil \log \frac{\delta_R}{\delta_D \left(\frac{\alpha}{\mu - \alpha}\right)} \middle/ \log \frac{\lambda_i^C}{\lambda_i^C + \mu} \right\rceil.$$

*Proof.* The proof appears in Appendix A.2. □

One of the most significant implications of Theorem 1 is that the sharing threshold does not depend on the demand rate of the external population. Moreover, the threshold is not linearly proportional to the internal camp demand rate.

As the sharing threshold represents the point at which costs transition, we next employ the threshold values  $\Omega_i$  to represent the expected total cost for each camp  $i$ , which is the sum of expected referral, deprivation, and holding costs.

**Theorem 2.** *Using the sharing threshold obtained in Theorem 1, the expected total cost for camp  $i$  with an inventory of  $X_i$  is:*

$$E[C^T(X_i)] = \gamma_1(\cdot)\gamma_2(\cdot)^{X_i} + hX_i/\mu + \gamma_3(\cdot), \quad (2)$$

where the component functions depend on input parameters and whether allocation  $X_i$  exceeds threshold  $\Omega_i$ . These component functions are summarized as follows:

$$\gamma_1(\cdot) = \begin{cases} \left( \frac{\lambda_i^C + \lambda_i^U + \mu}{\lambda_i^C + \lambda_i^U} \right)^{\Omega_i} \left[ \lambda_i^U \left( \frac{h}{\mu^2} + \frac{\delta_R}{\mu} \right) + \lambda_i^C \left( \frac{\lambda_i^C}{\lambda_i^C + \mu} \right)^{\Omega_i} \left( \frac{h}{\mu^2} + \delta_D \left( \frac{\alpha}{\mu - \alpha} \right) \right) \right] & \text{if } X_i > \Omega_i, \\ \left( \delta_D \lambda_i^C \left( \frac{\alpha}{\mu - \alpha} \right) + \frac{h\lambda_i^C}{\mu^2} \right) & \text{otherwise;} \end{cases} \quad (3)$$

$$\gamma_2(\cdot) = \begin{cases} \frac{\lambda_i^C + \lambda_i^U}{\lambda_i^C + \lambda_i^U + \mu} & \text{if } X_i > \Omega_i, \\ \frac{\lambda_i^C}{\lambda_i^C + \mu} & \text{otherwise;} \end{cases} \quad (4)$$

$$\gamma_3(\cdot) = \begin{cases} \frac{h}{\mu^2} (-\lambda_i^C - \lambda_i^U) & \text{if } X_i > \Omega_i, \\ \frac{\lambda_i^U \delta_R}{\mu} - \frac{h\lambda_i^C}{\mu^2} & \text{otherwise.} \end{cases} \quad (5)$$

*Proof.* The proof appears in Appendix A.3. □

We use Theorems 1 and 2 to construct the essential mathematical optimization problem we employ in making aid allocation decisions, which is now presented.

### 4.3 Nonlinear Aid Allocation Optimization Model

As expressed in Theorem 2, the total cost function for each individual camp is the sum of the respective expected referral, deprivation, and holding costs, as well as the holding costs for unallocated aid in the distribution center. We now seek to determine the optimal order up to levels  $\mathbf{X}$  that a central decision-maker should target to minimize the expected total cost to the refugee camp system. From this point onward, while the decision variables  $X_i$  representing units of aid are technically integer, given the relatively large demand values we make the modest assumption to relax these variables to continuous for the sake of improved managerial analysis.

Our nonlinear optimization model seeks to allocate aid to refugee camps in a manner that minimizes the expected total cost to the system:

$$\min_{\mathbf{X} \geq \mathbf{I}} E[C^T(\mathbf{X})] = \sum_{i=1}^N \gamma_1(\cdot) \left[ \gamma_2(\cdot) \right]^{X_i} + \sum_{i=1}^N \gamma_3(\cdot) + h/\mu \left( \mathcal{S} + \sum_{i=1}^N I_i \right), \quad (6a)$$

$$\text{subject to } \sum_{i=1}^N (X_i - I_i) \leq \mathcal{S}. \quad (6b)$$

Nonnegative value  $X_i - I_i$  is the amount to be shipped to camp  $i$ . The last term in the objective function indicates, upon total shipment quantity of  $\sum_{i=1}^N (X_i - I_i)$  units, that unallocated inventory exists in the amount of  $\mathcal{S} - \sum_{i=1}^N (X_i - I_i)$ . These items are expected to be kept for a duration of  $1/\mu$ .

Before considering solution approaches to nonlinear optimization problem (6), we note the following property regarding the objective function.

**Proposition 1.** *Objective function (6a) is continuous, that is, there is no discontinuity at the sharing threshold.*

*Proof.* The proof appears in Appendix A.4. □

The continuity of component functions as shown in Proposition 1 facilitates the optimization approaches in § 4.4.1 and § 4.4.2. We now analytically derive the solution to nonlinear optimization problem (6) when the relationship between allocation levels and respective sharing thresholds are known in advance for each camp.

## 4.4 Determining Optimal Aid Allocation

In this section we develop two methods for determining the optimal allocation of aid to refugee camp systems. We first analytically derive optimal allocation levels when there is an understanding of the optimal allocation with respect to the sharing threshold at each camp. The second method, which is more general, makes no such assumption, instead embedding piecewise linear approximation techniques in an optimization model to derive optimal allocation levels.

### 4.4.1 Optimal Allocations Under Known Allocation-Threshold Relationships

When the order up to level for each camp is a priori known to be either above, equal to, or below the sharing threshold, we analytically derive optimal order up to levels. Such closed-form results are particularly useful in the context of an unconstrained environment and abundance of supply to be distributed, where each camp will reasonably exceed its respective threshold. The closed-form solutions may also prove useful when there are certain restrictions in place concerning allocation levels and respective thresholds. For the sake of flow we include the derivations in their entirety in Appendix B. That said, while promising, the approach requires an initial feasibility assertion that is not guaranteed. Thus, we now provide a more general solution approach.

### 4.4.2 Piecewise Linear Approximation for Optimal Aid Allocation

The techniques in § 4.4.1 and Appendix B are useful to derive optimal order up to levels for optimization problem (6) under *known* relationships between the allocation  $X_i$  and sharing threshold  $\Omega_i$  for each camp  $i$ . This distinction is precisely how the piecewise components of the cost functions  $\gamma_1$ ,  $\gamma_2$ , and  $\gamma_3$  are defined in Theorem 2 of § 4.2: whether  $X_i$  exceeds threshold

$\Omega_i$  in each camp  $i$ . Hence, when the relationship between each  $X_i$  and  $\Omega_i$  is a priori unknown, an alternative method is needed to solve optimization problem (6); we now propose a piecewise linear representation of nonlinear objective function (6a).

Representing nonlinear objective function (6a) in a piecewise linear manner provides a distinct advantage: by discretizing the domain into a (possibly large, yet) finite number of breakpoints per camp  $i$ , each domain breakpoint has a known relationship with sharing threshold  $\Omega_i$ , and thus corresponding cost function evaluation. Moreover, by increasing the number of break points, we can approximate the piecewise expected total cost function within any degree of accuracy. We use the multiple choice model (see, e.g., Vielma et al., 2010) to implement our piecewise linear representation, and present notation as follows.

**Parameters.** We introduce notation for each camp  $i$ . Let  $B_i$  be the number of all linear segments of cost functions  $\gamma_1$ ,  $\gamma_2$ , and  $\gamma_3$ . The number of breakpoints is therefore  $B_i + 1$ . Let the domain of  $X_i$  be partitioned into equal-sized intervals from its lower bound to its upper bound. Denote the value of  $X_i$  at breakpoint  $j$  as  $b_i^j$ . The allocation cost for breakpoint  $b_i^j$  is thus calculated via lookup in objective function (6a) and the relationship of  $b_i^j$  with  $\Omega_i$ . The slope  $m_i^j$  and the intercept  $c_i^j$  of segment  $j$  are defined as:

$$m_i^j = \frac{\gamma_1(\cdot)(\gamma_2(\cdot))^{b_i^j} - \gamma_1(\cdot)(\gamma_2(\cdot))^{b_i^{j-1}}}{b_i^j - b_i^{j-1}} \quad i = 1, \dots, N, \quad j = 1, \dots, B_i, \quad (7)$$

$$c_i^j = \gamma_1(\cdot)(\gamma_2(\cdot))^{b_i^j} + \gamma_3(\cdot) - m_i^j b_i^j \quad i = 1, \dots, N, \quad j = 1, \dots, B_i. \quad (8)$$

Note that the relationship between  $b_i^j$  and  $\Omega_i$  directly informs the choice of piecewise cost components to use in (7) and (8), as per Theorem 2.

**Variables.** For each camp  $i$ , we introduce a set of binary variables  $V_i^j$ , where  $V_i^j = 1$  indicates that  $X_i$  is in interval  $j$ , and 0 otherwise. For each camp  $i$ , let variable  $Y_i^j$  equal  $X_i$ , if  $X_i$  is in the interval  $j$ , and 0 otherwise. Continuous variable  $Z_i$  denotes the piecewise linear approximation of the cost function for each camp  $i$ .

With this notation, we present our piecewise linear representation for optimal aid allocation.

$$\text{Minimize } \sum_{i=1}^N Z_i + h/\mu \left( \mathcal{S} + \sum_{i=1}^N I_i \right) \quad (9a)$$

$$\text{subject to: } \sum_{i=1}^N (X_i - I_i) \leq \mathcal{S}, \quad (9b)$$

$$\sum_{j=1}^{B_i} V_i^j = 1 \quad i = 1, \dots, N, \quad (9c)$$

$$b_i^{j-1} V_i^j \leq Y_i^j \leq b_i^j V_i^j \quad i = 1, \dots, N, \quad j = 1, \dots, B_i, \quad (9d)$$

$$\sum_{j=1}^{B_i} Y_i^j = X_i \quad i = 1, \dots, N, \quad (9e)$$

$$\sum_{j=1}^{B_i} (m_i^j Y_i^j + c_i^j V_i^j) = Z_i \quad i = 1, \dots, N, \quad (9f)$$

$$X_i \geq I_i \quad i = 1, \dots, N, \quad (9g)$$

$$Y_i^j \geq 0 \quad i = 1, \dots, N, \quad j = 1, \dots, B_i, \quad (9h)$$

$$Z_i \in \mathbb{R} \quad i = 1, \dots, N, \quad (9i)$$

$$V_i^j \in \{0, 1\} \quad i = 1, \dots, N, \quad j = 1, \dots, B_i. \quad (9j)$$

Objective function (9a) sums the piecewise approximations  $Z_i$  over each camp, together with the (fixed) holding costs. Constraint (9b) ensures that allocations stay within the limits of total supply. Constraint sets (9c) and (9d) work together to collectively ensure that exactly one segment is activated for each camp, and for that activated segment, the value of  $Y_i^j$  assumes a value between its breakpoints. Constraint set (9e) assigns  $X_i$  to this value, while constraint set (9f) assigns the piecewise approximations  $Z_i$  for each camp based on the activated slope and intercept terms. Variable domains are represented in (9g)–(9j).

As optimization model (9) determines the optimal  $\mathbf{X}$  that minimizes the expected total cost to the system within any degree of accuracy, it can be used to optimally allocate aid to the entire refugee camp system under the derived sharing thresholds from Theorem 1. Note that a side outcome is that it prescribes a relationship between  $X_i$  and  $\Omega_i$ , which can reconcile with the optimality conditions presented in § 4.4.1. Moreover, we provide open source code for the implementation of optimization model (9) so that researchers in the field can put into practice the results of the model, given respective input.

## 5 Computational Studies with Real and Synthetic Data

In this section we conduct computational studies to understand the performance of our mathematical modeling. We begin by investigating the performance on a case study motivated by real data in the context of distributing medicine to Syrian refugee camps in Turkey, and subsequently discuss managerial insights related to our findings. We then turn to synthetic data to more fully understand the inherent tradeoffs in this aid allocation problem by considering a greater number of refugee camps, and offer further managerial insights associated with larger instances. We evaluate our results through an extensive simulation study across several varied key parameters and distributions.

## 5.1 Experimental Design

We now detail how we conduct our computational studies, including the parameter estimation and setup for our case study of the Syrian refugee camps in Turkey, as well as for synthetic data. The inputs include the deprivation coefficient, deprivation rate, referral cost for unmet external demand, holding cost per time unit, and rate for exponentially distributed time between replenishment cycles. While we would welcome as much real data as possible for estimation, the reality is that there is limited access to precise parameter estimates, with no established standard. We therefore use various parameters sourced from the humanitarian and healthcare literature where necessary (see, e.g., [Beamon and Kotleba \(2006a\)](#) and [Roni et al. \(2016\)](#)). We further supplement our baseline derivations that rely on exponentially distributed replenishment cycles through an extensive simulation that appears in [Appendix C](#).

For simplicity in cost calculations, we assume an annual holding cost of one, and define other cost parameters in multiples of this unit holding cost. We incentivize greater sharing in our model by considering that one referral is twice as costly as keeping a unit for a year in inventory. We more heavily penalize deprivation, where the annual holding cost for a unit is approximately equivalent to being deprived for less than a year, such as one month (12 per year). For a deprivation rate  $\alpha$  and an internal refugee waiting time  $T$ , the deprivation coefficient  $\delta_D$  is thus set to a value that permits satisfying the deprivation cost of unmet demand of duration  $T$  to be approximately equal to an annual holding cost of one, that is:  $\delta_D(e^{\alpha T} - 1) \approx 1$ . The respective choices of referral cost and deprivation coefficient also ensure the inequality  $\delta_R < \delta_D(\frac{\alpha}{\mu - \alpha})$  holds for every combination of  $\alpha$  and  $\mu$  values used in our testing.

The size of  $\mathcal{S}$  determines the total number of breakpoints for piecewise linear formulation (9). For each camp, we place an initial breakpoint at the threshold level  $\Omega_i$  to better approximate the expected total cost in equation (2), and evenly space remaining breakpoints above this threshold, and below (until zero). The method to compute the number of breakpoints is formalized in the respective experiments.

All experiments are run on parallel computing resources with 1 node, and 8 cores per node. We use Gurobi Optimizer version 8.0.4 ([Gurobi, 2020](#)) with Python 3.6.5 interface for solving optimization model (9). We use default Gurobi parameter settings for all of our experiments. These details provide the backdrop for testing our approaches under two cases: 1) a case study involving real data from Syrian refugee camps in Turkey, and 2) synthetic data.

## 5.2 Distributing Aid to Syrian Refugee Camps in Turkey: A Case Study

With nearly 3.7 million refugees, Turkey hosts by far the largest number of refugees worldwide ([IOM, 2019](#)), mainly from Syria. Indeed, more than half of the displaced Syrian population currently resides in Turkey ([UNHCR, 2019](#)). Turkey provides a substantial proportion of the financial support for these refugee populations. Moreover, the publicly-funded healthcare system in Turkey provides for not only its citizens, but also for those with refugee status, thereby impacting the welfare of its own citizens. Indeed, while access to proper healthcare services remains a common challenge faced by refugees ([Lam et al., 2015](#); [Terefe, 2017](#)), many Syrian refugees do visit public Turkish hospitals for their healthcare needs ([Ekmekci, 2016](#)). Over the past decade, the government has continued to care for camp-based as well as the significant urban refugee populations surrounding these camps.

On average, more than 98% of refugees in Turkey reside *outside* of camps ([Turkish Refugee Association, 2020](#)). Among camp-based refugees, 94% of women and 90% of men have access to immediate health services, whereas only 56% of female and 60% of male urban refugees have

immediate access to health services ([Republic of Turkey Prime Ministry Disaster and Emergency Management Authority, 2014](#)). The majority of the overall population in these areas is now composed of Syrians, and nearly half are minors, requiring a significant amount of humanitarian aid such as medicine ([UNHCR, 2019](#)). Given that refugees are predominantly urban and in need of access to health care, having their needs satisfied in camp would also reduce the burden on local hospitals.

Border locations in Turkey that host Syrian refugees include Hatay, Adana, Kilis, Kahramanmaraş, and Osmaniye. Each of these areas have at least one camp (Hatay has three). For these five areas, Table 5 provides details on the number of camp-based ([UNHCR, 2020](#)) and urban ([Ministry Interior of Turkey, 2020](#)) refugees and associated demand rates existing in the seven camps. Note that to differentiate the three camps in Hatay, we manually divided its internal refugee population using an approximate 20%, 30%, and 50% split. We compute the internal (external) annual demand rate using 20% (2%) of the internal (external) population size.

In addition to these  $N = 7$  camps, for the case study we assume a holding cost per time unit of 1, a referral cost  $\delta_R$  of 2, and a replenishment cycle rate  $\mu$  of 2 per year. Additionally, we assume the annual holding cost for a unit is approximately equivalent to being deprived for 24 days (15 per year) for deprivation rate  $\alpha = 0.75$  per year. Thus, the deprivation coefficient  $\delta_D$  is set to 20, satisfying  $\delta_D(e^{0.75/15} - 1) \approx 1$ . We also assume initial inventory levels  $I_i = 0$  for all camps.

Table 5: Refugee Populations and Demand Rates for Turkish Areas with One or More Camps.

Area	Refugee Population			Annual Demand Rate		
	Total	Internal	External	Total	Internal	External
<b>Hatay 1</b>	438,741	2,142	144,105	3,310	428	2,882
<b>Hatay 2</b>		3,213	143,034	3,504	643	2,861
<b>Hatay 3</b>		5,355	140,892	3,889	1,071	2,818
<b>Adana</b>	246,462	21,414	225,048	8,784	4,283	4,501
<b>Osmaniye</b>	49,544	12,418	37,126	3,227	2,484	743
<b>Kilis</b>	112,192	8,492	103,700	3,772	1,698	2,074
<b>Kahramanmaraş</b>	92,293	10,872	81,421	3,802	2,174	1,628

We solve optimization model (9) for the above parameters by varying levels of total supply  $\mathcal{S}$ . Piecewise linear segments are generated so that the difference between each consecutive breakpoint is 2 units. As  $\mathcal{S}$  varies, the number of breakpoints varies between 2,016 and 158,172. All instances are solved to global optimality via [Gurobi \(2020\)](#) in under one minute.

### 5.3 Managerial Insights from Syrian Refugee Case Study in Turkey

We now discuss insights obtained by experimentation on the Syrian camp system in Turkey using the parameter levels detailed in § 5.2. Figure 2 shows the optimal allocation across increasing values of  $\mathcal{S}$  while holding other model parameters fixed, where each level of  $\mathcal{S}$  corresponds to a specific instance of optimization model (9). The  $x$ -axis shows the total allocable supply  $\mathcal{S}$  to be distributed among all camps by the central decision-maker, and the  $y$ -axis displays the optimal allocation of camps for different levels of  $\mathcal{S}$ . For each level of  $\mathcal{S}$ , we plot the optimal allocation values  $X_i$  per camp  $i$ . Doing so over many levels of  $\mathcal{S}$  creates contours that show the total amount supplied versus the optimal allocation levels for each camp. Each contour line has

three types of markers: (1) small markers indicating levels of  $\mathcal{S}$  for which the optimal allocation for a camp is no more than the sharing threshold for that camp; (2) An empty circle indicating the sharing threshold value for each camp; and (3) large markers indicating that the optimal aid allocation exceeds the threshold for that camp, when optimal allocation begins to also satisfy urban demand.

The right panel of Figure 2 depicts pie charts for each camp, where the radius of each chart reflects the corresponding total demand rate for that camp. The camps appear in descending order of total demand rate, beginning with Adana through the smallest, Osmaniye. Each pie chart reveals the proportion of the internal demand rates to the external demand rates for the corresponding camp, and readily show how the camps differ with regard to these aspects.

**Insight 1.** *Internal demand rate appears as a key driver of allocation decisions for lower levels of the total allocable supply.*

As can be seen in Figure 2, Adana is the largest camp and Hatay 1 is the smallest camp in terms of internal demand rate  $\lambda_i^C$ . The internal demand rate appears as a key driver of the initial allocation decisions, so that the optimal aid allocated to Adana exceeds the other camps for all levels of total supply, whereas the optimal allocation of Hatay 1 always trails the others. The reason for this behavior is that the expected cost of unsatisfied internal demand (that is, the deprivation cost) is relatively high, and therefore each camp prioritizes the satisfaction of its own internal demand. The behavior of the internal demand rate as the main driver of the allocation decisions can shift as the total allocable supply increases. This is evident in Figure 2 when observing higher levels of total supply, in particular for Osmaniye and Kahramanmaraş. While Osmaniye has a higher internal demand rate than Kahramanmaraş, the optimal allocated aid to Kahramanmaraş becomes larger than Osmaniye from the point that total supply exceeds approximately 32,600 units.

**Insight 2.** *When total supply is below the transition zone, allocations are driven by the internal demand rate, whereas total supply above the transition zone has allocations driven by the total demand rate. In between, the transition zone features uncertain allocations.*

Figure 2 shows that as the total supply increases, the optimal allocation for each camp increases with approximately constant slope below and above the *transition zone* – the grey vertical region that is driven largely by the dynamic and uncertain interactions between camps as they reach their sharing thresholds. Note that this transition zone is fairly narrow with respect to the depicted domain of total supply levels, no more than 10%. Therein, the piecewise cost functions introduced in Theorem 2 undergo a transition for each camp  $i$ , as the optimal allocation ( $X_i$ ) with respect to total supply increases begin to exceed threshold values ( $\Omega_i$ ). The increasing behavior of optimal allocations within this zone undergoes a transition, starting from a total supply value of around 11,500, near where the first camp achieves its sharing threshold.

A key question that arises in this context is: *how should an additional unit of aid be allocated?* Figure 3 reveals insights into this question. The left panel depicts the setting below the transition zone, while the right panel depicts above the zone. For both panels, camp names appear along the  $x$ -axis, against the left  $y$ -axis of demand rate, and the right  $y$ -axis of percent of allocated aid. The camps are intentionally ordered on the  $x$ -axis according to their fraction of allocated aid, so as to reveal most likely contributing factors to the allocation. It can be clearly seen that the most important criteria for allocating aid to the camps is the internal demand rate below the transition zone; whereas above the zone, the optimal allocations are more proportional to the total demand rate, as can be reasoned from Theorem 2.

Figure 2: Computational Results For Turkish Case Study. Left Panel: Optimal Allocation for Various Levels of Total Supply; Right Panel: Internal, External, and Total Camp Demand Rates.

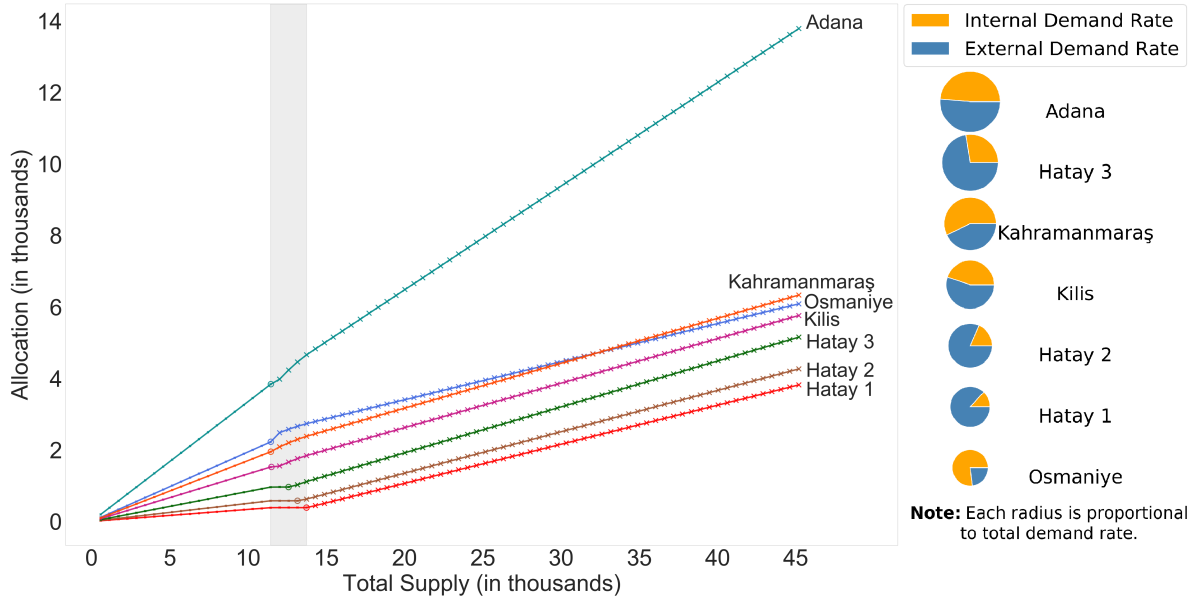


Figure 3: The Optimal Allocation of Aid as the Fraction of Aid Allocated to Each Camp.

(a) Below the Transition Zone.

(b) Above the Transition Zone.

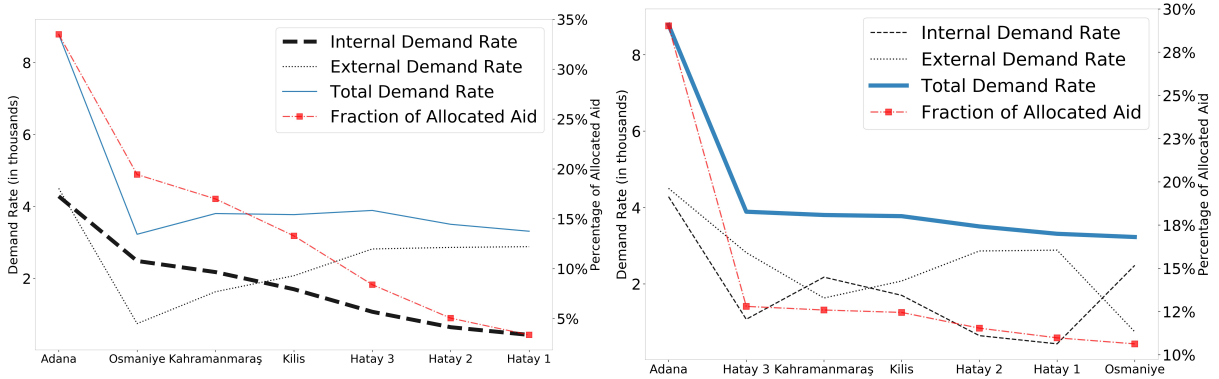
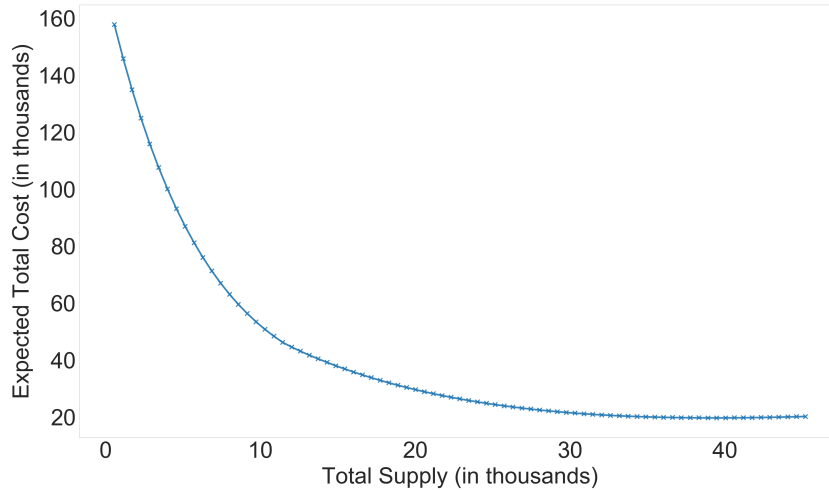


Figure 4 plots the minimized expected total cost on the  $y$ -axis as a function of the total allocable supply  $\mathcal{S}$  along the  $x$ -axis, while other parameters are fixed in optimization formulation (9). Note that the total supply is not a decision variable over which we optimize; rather, total supply is a fixed parameter, and for each level of  $\mathcal{S}$  there is a corresponding point plotting the total system cost (over all camps) obtained from solving optimization model (9). As can be seen in Figure 4, higher levels of supply result in lower expected total costs because of the significant deprivation and referral costs that occur at lower supply levels, beyond the more traditional holding costs. Even so, at very high levels of supply, the total cost will eventually increase as inventory cost contributions begin to outweigh the decrease in other costs.

Figure 4: Objective Function Versus Total Supply.



#### 5.4 Experimental Parameters for Synthetic Data

We generate synthetic data instances to measure the performance of our optimization model and solution approach. In particular, we create 16 instances by varying key model parameters such as number of camps (4 levels), annual replenishment cycle rate (2 levels), and deprivation rate (2 levels). Each instance is named according to the convention “*Number of camps–Annual replenishment cycle rate–Deprivation rate*” to show the considered levels of these parameters. Table 6 contains the parameters and associated values used for creating our synthetic instances.

Table 6: Summary of Data Used in Synthetic Computational Experiments.

Instance Code	Deprivation Coefficient ( $\delta_D$ )	Referral Cost ( $\delta_R$ )	Holding Cost per Time Unit ( $h$ )	Number of Camps ( $N$ )	Replenishment Cycle Rate ( $\mu$ )	Deprivation Rate ( $\alpha$ )
5-6-0.25					6	0.25
5-6-0.75	50	2	1	5		0.75
5-1-0.25					1	0.25
5-1-0.75						0.75
10-6-0.25					6	0.25
10-6-0.75	50	2	1	10		0.75
10-1-0.25					1	0.25
10-1-0.75						0.75
20-6-0.25					6	0.25
20-6-0.75	50	2	1	20		0.75
20-1-0.25					1	0.25
20-1-0.75						0.75
50-6-0.25					6	0.25
50-6-0.75	50	2	1	50		0.75
50-1-0.25					1	0.25
50-1-0.75						0.75

We vary the number of camps  $N$  in the set  $\{5, 10, 20, 50\}$  to evaluate the effect of the network size on model tractability. For each level of  $N$ , we assume that half of the camps are small, with annual internal demand rates uniformly distributed between 2,500 and 10,000, and surrounding population demand rates between 1,000 and 5,000. Similarly, for large camps we assume uniform

annual internal demand rates between 10,000 and 20,000, and annual surrounding population demand rates between 15,000 and 30,000. We include two values for the annual replenishment cycle rate. For half of the instances, we assume a (yearly) replenishment rate of 6 for cycles, implying an expected length of two months. Thus these instances will feature more frequent replenishments than the remaining instances, where the replenishment rate is taken as 1, implying an expected length of 1 year for cycles. Finally, we include two deprivation rates, 0.25 and 0.75. We set initial inventory levels  $I_i = 0$  for all camps, the effect of which is that the order up to levels are equal to the actual amount shipped. This has the benefit of making the actual pattern of aid distribution transparent, eliminating effects such as a camp with an anomalous high initial inventory level skewing the distribution pattern.

For simplicity in cost calculations, we similarly assume an annual holding cost of one, and define other cost parameters in multiples of this unit holding cost. We incentivize greater sharing in our model by considering that one referral is twice as costly as keeping a unit for a year in inventory. Deprivation is more heavily penalized, with the annual holding cost for a unit is approximately equivalent to being deprived for one month (12 per year) and ten days (36 per year), for rates of 0.25 and 0.75, respectively. The deprivation coefficient  $\delta_D$  is thus set to 50, satisfying both  $\delta_D(e^{0.25/12} - 1) \approx 1$  and  $\delta_D(e^{0.75/36} - 1) \approx 1$ . The selected levels of 2 and 50 for referral cost and deprivation coefficient, respectively, also ensure the inequality  $\delta_R < \delta_D(\frac{\alpha}{\mu - \alpha})$  is maintained for all combinations of  $\alpha$  and  $\mu$  values used in our testing.

## 5.5 Synthetic Data: Model Performance and Additional Managerial Insights

We now demonstrate the performance of optimization model (9) on the synthetic data instances introduced in Table 6 across various levels of total supply  $\mathcal{S}$ , and discuss key insights gleaned from the results. We consider the length of the piecewise linear segments in proportion to the total supply  $\mathcal{S}$ . The difference between consecutive breakpoints is set to one of the following values: (a) 2, if  $\mathcal{S}$  is less than or equal to 50,000; (b) 10, if  $\mathcal{S}$  is between 50,000 and 500,000; or (c) 50, if  $\mathcal{S}$  is greater than or equal to 500,000. This procedure of generating piecewise line segments results in the number of breakpoints varying between 155 and 3,000,000. Correspondingly, this impacted the Gurobi build and solve times for the corresponding optimization problems: from a minimum of under one second for smaller instances, and up to 90 minutes for the largest.

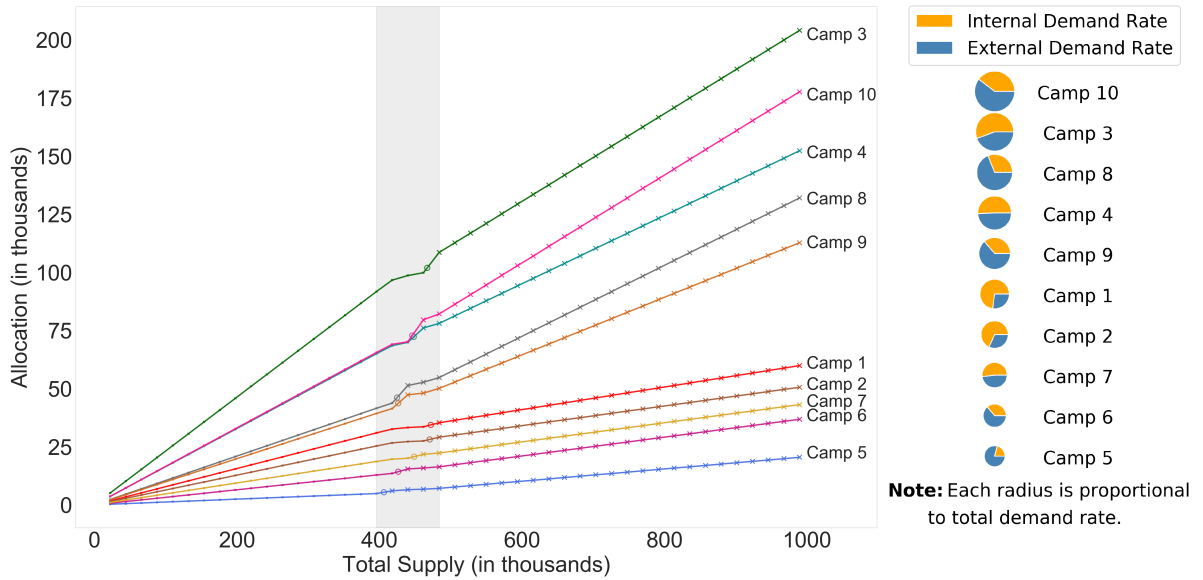
The pattern of optimal allocation exhibits similar overall behavior for all instances, such as instance *10-1-0.75* which is depicted in Figure 5. In general, there is an observable trend that is not dissimilar to our case study instance: as the total supply increases, aid is allocated across the camps in an increasing manner, though at somewhat different rates due to the interplay of the internal, external, and total demand rates across camps. As total supply increases *at lower levels*, the optimal allocation for all camps increases with an approximately constant, positive slope. This trend continues until the first camp reaches its sharing threshold, at which time the curious behavior of the *transition zone* emerges. In this narrow zone, frequent transitions reign with respect to optimal allocations as the dynamics between internal, external, and total demand rates of camps create tension among the individual allocations. This pattern continues until the last camp reaches its sharing threshold, after which a new steady state is soon reached, and optimal camp allocations again stabilize and increase with an approximately constant slope (though often distinct from pre-zone slopes).

These behaviors are visualized in Figure 5, with the transition zone appearing as a grey vertical region. The camp with the highest proportion of external-to-internal demand rate, camp 5, is the first to reach its threshold, around total supply of 400,000. Prior to this, the trend of increasing optimal allocation is similar across camps. After reaching this level, however,

transitions dominate the optimal allocation patterns, until a new steady state is reached around total supply of 475,000. The transition zone reflects the relative costs of different camps as shaped according to the particular model parameter settings (such as demand rates and other settings as per Table 6).

We draw the attention of the reader to a specific behavior that illustrates the way that internal, external, and total demand rates influence expected total costs. In Figure 5, the optimal allocations for camp 4 and camp 10 nearly coincide up until they reach their sharing thresholds, around total supply levels of 440,000. Beyond that point, the optimal allocation for camp 10, which is larger in terms of total demand rate, exceeds that of camp 4. Indeed, their internal demand rates are nearly identical, causing their pre-threshold costs to track in parallel; beyond the threshold, the cost function behavior transitions in a distinct manner due to the larger external demand rate of camp 10 contributing more to the referral cost. To a lesser degree, a similar behavior is also observed in camps 8 and 9.

Figure 5: Computational Results for Instance with 10 Camps, Replenishment Cycle Rate  $\mu = 1$  per year, and Deprivation Rate  $\alpha = 0.75$  per year ( $10-1-0.75$ ); Right Panel: Demand Rates.



Additional insights are apparent by comparing the results of Figure 5 with either Figure 6 (varying the annual replenishment cycle rate) or Figure 7 (varying the deprivation rate), while holding all other parameters constant (including the number of camps  $N = 10$ ).

**Insight 3.** *At lower levels of deprivation rate  $\alpha$ , external demands are accepted at lower levels of total supply.*

Instances  $10-1-0.75$  and  $10-1-0.25$  are depicted in Figures 5 and 6, respectively, differing only in deprivation rate  $\alpha$ . As compared to the distributions in Figure 5, it can be seen in Figure 6 that all camps reach their sharing thresholds at lower levels of total supply  $\mathcal{S}$ , noting the differences in the  $x$ -axis scale. This occurs because instance  $10-1-0.25$ , which has the lower deprivation rate, has correspondingly lower costs of unsatisfied internal demand; thus, its camps start accepting external demand at earlier levels of total supply. In all other aspects, the optimal allocation behavior over all supply levels is identical, with the same ordering and relative allocation ratios across all camps.

Figure 6: Optimal Allocation Versus Various Levels of Total Supply for Instance  $10-1-0.25$ .

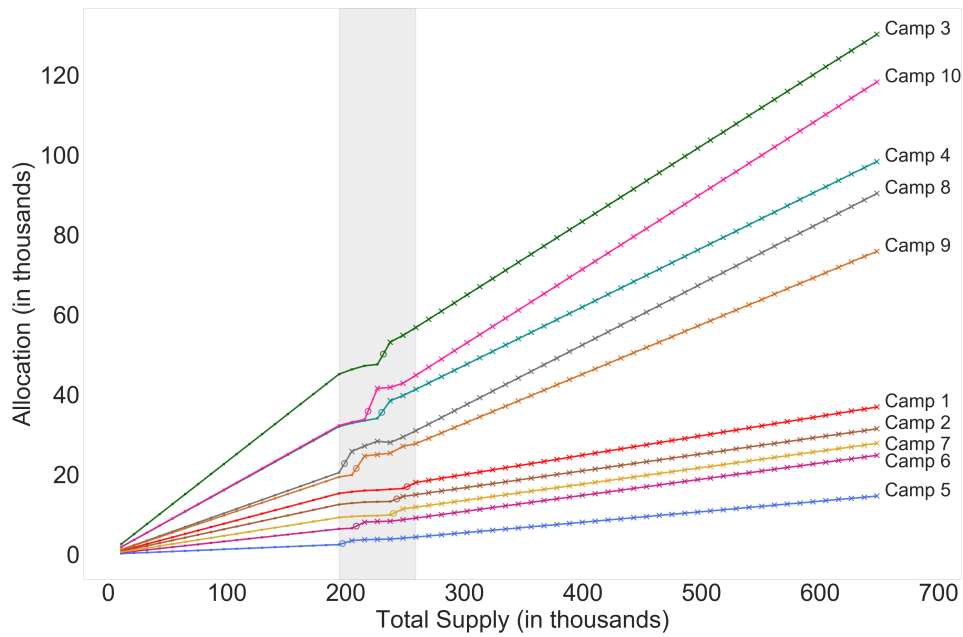
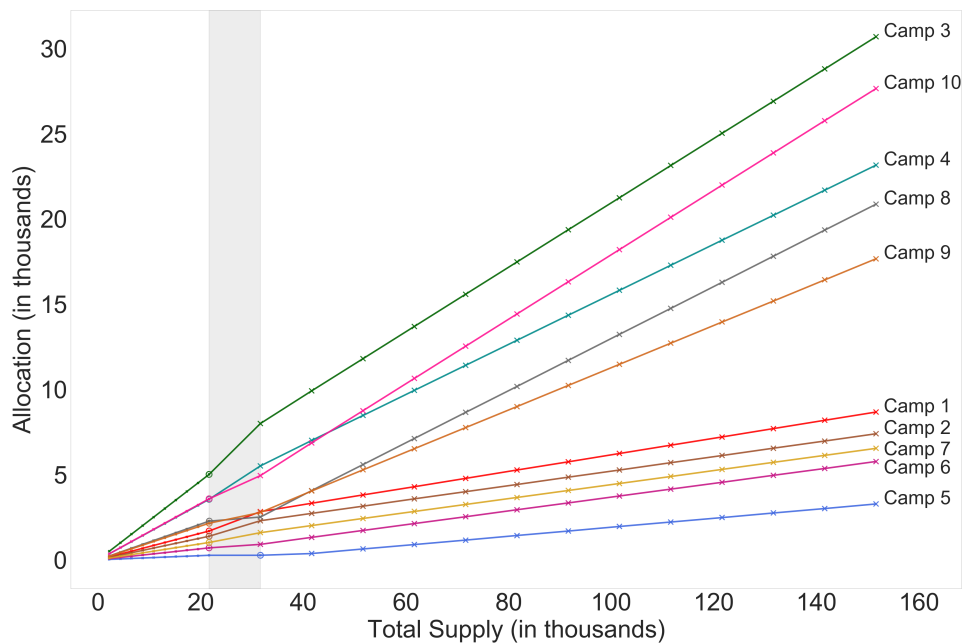


Figure 7: Optimal Allocation Versus Various Levels of Total Supply for Instance  $10-6-0.75$ .



**Insight 4.** Shorter expected replenishment durations tend to permit sharing of aid with urban refugees at lower levels of total supply.

In a similar manner, instances  $10-1-0.75$  and  $10-6-0.75$  are depicted in Figures 5 and 7, which differ only in annual replenishment cycle rate  $\mu$ . The camps in Figure 7 reach their sharing threshold earlier because the risk of having unsatisfied demand is lower with shorter replenishment cycles. This causes camps to start satisfying external demands earlier in Figure 7, which

depicts instance  $10-6-0.75$ . Outside of this exception, the increasing allocation trends and camp orderings are largely identical to that of instance  $10-1-0.75$  depicted in Figure 5.

## 6 Concluding Remarks

Our study investigates the optimal allocation of aid under uncertainty in refugee camp systems. We consider uncertainty in demand for a homogeneous type of aid from both *camp-based* (internal) and *urban* (external) refugee populations, as well as uncertainty in replenishment cycle duration, and develop sharing thresholds whereby aid should be shared with external populations, or reserved for internal populations. We use these thresholds to construct cost functions that quantify three costs: the cost of referring external populations elsewhere, the cost of holding excess inventory in the system, and the cost of depriving internal refugee populations, which places value on human suffering. We then optimize over the combined cost functions for the entire camp system to determine optimal order up to (target) levels that minimizes overall camp system cost. Our modeling, while necessarily somewhat stylized for tractability, yields a variety of managerial insights arising from solving our problem both for synthetic data, as well as real data from the Syrian refugee camp system in southern Turkey. We validate our baseline derivations that rely upon exponentially distributed replenishment cycles via an extensive simulation (Appendix C). While for a small minority of runs some discrepancies exist with respect to total costs, the overall results of our simulation reveal broad support for the generalization of our optimal thresholds and allocations across varied key parameters and distributions. Our findings demonstrate how to allocate limited aid resources to refugee camp systems under uncertain demand and replenishment cycle duration, such as the Syrian refugee crisis in Turkey.

In light of this framework, we recommend that humanitarian aid be distributed from a central decision-maker to a refugee camp system as follows. Three general states exist from the viewpoint of the total allocable supply of aid. For the first, which is in effect for lower levels of total supply, aid allocation should be made so as to prioritize camps with the largest internal demand rate. For the last, in effect for higher levels of total supply, aid allocation should be made so as to prioritize camps that have the largest total (internal plus external) demand rate. In between these two states with steady patterns, a relatively narrow *transition zone* exists. In this zone, camp aid allocation patterns undergo frequent shifts due to underlying internal, external, and total demand rate dynamics. These behaviors are driven by individual camp allocations reaching their sharing thresholds, which govern when camps stop reserving aid solely for internal, camp-based refugees, and begin sharing with nearby urban refugee populations. Thus, for total supply levels that are within the transition zone, the results of our optimization model will yield accurate aid allocation recommendations.

Properly designed allocation models for critical aid have great potential to ensure timely satisfaction of demand in complex emergencies such as extenuated refugee camp system settings. Our study is positioned among the growing body of literature that explicitly integrates deprivation costs into the objective function (see, e.g., [Holguín-Veras et al., 2013, 2016](#); [Gutjahr and Fischer, 2018](#); [Shao et al., 2020](#)). One of the most significant implications of our study, via Theorem 1, is that the derived sharing threshold values do not depend on the demand rate of the surrounding population. Moreover, the threshold is not linearly proportional to the internal camp demand rate. Further, a unique benefit of our approach is that we can set an inventory threshold level that benefits both primary and secondary populations. By satisfying requests from external camp populations when possible, our approach benefits donor relations and related humanitarian concerns, in terms of using scarce resources accurately and in a timely manner. While the focus of our case study is the allocation of medicine to Syrian refugee camps in Turkey,

our modeling is general to a variety of single-commodity allocation settings, and there are other post-disaster environments for which our modeling may be appropriate, where the demand and supply availability of nonperishables<sup>6</sup> are uncertain.

Practically speaking, piecewise linear optimization formulation (9) can be solved very quickly, often in a matter of seconds, via the commercial solver [Gurobi \(2020\)](#). Moreover, limited testing with the open-source optimization solver CBC ([COIN-OR, 2020](#)) indicates great potential to solve even the largest of problems (dozens of camps and many thousands of breakpoints) within a few hours, thereby posing no barrier to solving a challenging aid allocation problem in practice. Moreover, we provide open source code for our implementation via a Python script that uses the free PuLP ([Mitchell et al., 2020](#)) library to build the optimization model, calls the CBC solver<sup>7</sup> ([COIN-OR, 2020](#)) for solving, and generates corresponding allocation visualizations, thereby broadening the availability of our work to others in similar aid distribution settings. The source code is made freely available for download at the author’s website ([Trapp, 2021](#)).

Our study is not without limitations. We believe the generated uncertain parameters are realistic, including demand rates and replenishment cycle durations, and at the same time acknowledge that actual data would improve our insights, and that there may be other reasonably justified parameter values in related contexts. Our assumption that demand occurs in single unit requests may not be realistic in general; multiple units could instead be demanded simultaneously (e.g., number of painkillers provided depending on patient severity). Moreover, we assume *independent* camp-based and urban demands and *stationary* demand rates over the cycle duration in question, two months and six months in our study. While these assumptions provide a good foundation for future studies, they do not allow for the more focused analysis when rates of arrivals quickly change, such as during a fast-hitting pandemic, or when there are frequent surges of refugees. Surges are likely to affect urban demand differently than camp-based demand, and perhaps new camp construction, and if they were to occur with frequency greater than the cycle duration, this would also call for additional analysis.

There are a number of directions for future work. We consider a centralized decision-maker that allocates aid via a single warehouse distribution center to an existing refugee camp system; in practice, multiple agencies may distribute aid using the resources of an umbrella organization, such as UNJLC ([Balcik et al., 2010](#)). Coordination between multiple humanitarian agencies is a major challenge in managing refugee operations ([Dunn, 2016](#); [Karsu et al., 2019](#)), and policies for inventory control and sharing with multiple agencies are more complicated than the case of a single relief agency due to associated costs. We consider a single type of aid in our study, however humanitarian agencies usually allocate multiple commodities, with perhaps varying demand rates. Our model can accommodate the multi-commodity framework, if key model parameters are independent. While cost parameters for each commodity are typically independent, some supply and demand rates may be correlated, which would call for additional modeling in future work.

Related to the limitations above, it would be insightful to investigate threshold and allocation tendencies specific to non-stationary and perhaps correlated demand scenarios, using compound and nonhomogeneous Poisson processes. Moreover, considering more frequent refugee surges is an interesting avenue of future study, placing the context more in the emergency phase of refugee crises. The problem we consider may also benefit from a stochastic programming framework. In particular, initial allocation decisions could be hedged against the uncertainty in demand rates

---

<sup>6</sup>The model may also be applicable for certain perishable items like food and some pharmaceuticals, so long as they do not perish during the cycle time. However, this introduces other considerations such as queueing rules.

<sup>7</sup>While our implementation calls CBC by default, the choice of solver can be easily swapped with a commercial solver such as [Gurobi \(2020\)](#) or [CPLEX \(IBM, 2020\)](#), assuming appropriate licensing.

and replenishment cycle durations, leading to recourse decisions involving how to redistribute supplies among camps. An approach that uses transshipments of stock to share between camps, perhaps with distribution costs, would allow for more demand to be satisfied, though such an approach would likely require the generation of realistic demand scenarios.

## **Acknowledgments**

We are grateful for the assistance of many in making this research successful. In particular, Trapp and Azizi are grateful for the support of the National Science Foundation (Operations Engineering) grant CMMI-1825348, as well as that provided by the Foisie Business School at Worcester Polytechnic Institute.

## Appendix

### A Mathematical Proofs

We present detailed proofs related to sharing threshold and expected cost calculations in this section. As these results hold for every camp  $i$ , for ease of exposition we use  $X$  instead of  $X_i$ .

#### A.1 Proof of Lemma 1 (Expected Deprivation Cost for An Internal Refugee)

When a unit of aid is demanded with an initial inventory level of zero, we model the deprivation cost of a refugee waiting for an uncertain duration of time  $T$  as:

$$D(T) = \delta_D(e^{\alpha T} - 1). \quad (10)$$

Due to the memoryless property of the exponential distribution, the duration  $T$  that the refugee waits remains exponentially distributed with rate  $\mu$ . As  $T$  is a random variable, the expected deprivation cost per arrival becomes the expectation of a function of a random variable, which is computed as:

$$\begin{aligned} E[D(T)] &= \delta_D(E[e^{\alpha T}] - 1) = \delta_D\left(\int_0^\infty e^{\alpha t} \mu e^{-\mu t} dt - 1\right) \\ &= \delta_D\left(\int_0^\infty \mu e^{-(\mu-\alpha)t} dt - 1\right) \\ &= \delta_D\left(\frac{\mu}{\mu-\alpha} - 1\right) = \frac{\delta_D \alpha}{\mu-\alpha} \text{ for } \alpha < \mu. \end{aligned} \quad (11)$$

#### A.2 Proof of Theorem 1 (Sharing Threshold)

While a refugee camp system may contain many camps, the inventory management at each camp functions relatively independently, thus an inventory sharing threshold can be considered from the perspective of an individual camp. Thus, suppose that there is a single camp in the system. At the beginning of the cycle, which has an uncertain duration, the camp has a relatively high level of inventory. When an external (urban) refugee arrives to the camp to request aid, the question of concern is whether to accept the request or refer them elsewhere, to reserve inventory for internal (camp-based) refugees.

We model this inventory management problem as a probabilistic dynamic program (DP). At each inventory level (*state*), depending on the decision of whether to share, there are probabilistic outcomes.  $\Phi(X)$  denotes the expected cost of having  $X$  units of aid in inventory until the end of the cycle. The DP aims to solve  $\min \Phi(X)$ , where  $X$  is set to the initial units allocated. In order to compute a generic recursive relationship, we consider the following possible events leading to three alternative states:

- demand occurrence from an internal refugee,
- demand occurrence from an external refugee,
- a replenishment becomes available.

Random variables denoting the time until the next internal (external) refugee arrival are denoted by  $T_C$  ( $T_U$ ), where  $T_C \sim \text{Exponential}(\lambda^C)$  ( $T_U \sim \text{Exponential}(\lambda^U)$ ). Let  $W$  denote the cycle

duration, with  $W \sim \text{Exponential}(\mu)$ . Let  $\delta_D$  be the penalty incurred by the system when one unit of internal demand is not satisfied for a duration of one time unit, while  $\delta_R$  denotes the amount of penalty incurred by the system when an external demand is not satisfied. We assume  $\delta_D(\frac{\alpha}{\mu-\alpha}) > \delta_R$ , as otherwise the system would never refer, resulting in the trivial solution to share all aid.

The expected total cost of the system with  $X$  units of aid can be computed to reflect the generic recursive relationship as:

$$\begin{aligned} \Phi(X) = & 0 \cdot P(W = \min(T_C, T_U, W)) + \Phi(X-1)P(T_C = \min(T_C, T_U, W)) \\ & + \min\{\Phi(X-1), \delta_R + \Phi(X)\}P(T_U = \min(T_C, T_U, W)) \end{aligned} \quad (12)$$

$$= \Phi(X-1)\frac{\lambda^C}{\lambda^C + \lambda^U + \mu} + \min\{\Phi(X-1), \delta_R + \Phi(X)\}\frac{\lambda^U}{\lambda^C + \lambda^U + \mu}. \quad (13)$$

Note that if the inventory is replenished, the reached state incurs a cost of zero because the current cycle is has completed. If the next event in the system is an internal demand, the observed request has to be satisfied, and the state is decreased by one. If the next event in the system is an external demand, the observed request is either satisfied, or the request is referred elsewhere. The last term in (13) aims to compute the action with the minimum expected costs.

If the request from an external refugee is satisfied, then

$$\begin{aligned} \Phi(X) &= \frac{\lambda^C}{\lambda^C + \lambda^U + \mu}\Phi(X-1) + \frac{\lambda^U}{\lambda^C + \lambda^U + \mu}\Phi(X-1), \\ \Phi(X) &= \frac{\lambda^C + \lambda^U}{\lambda^C + \lambda^U + \mu}\Phi(X-1). \end{aligned} \quad (14)$$

Alternatively, if the external refugee is referred elsewhere, then

$$\begin{aligned} \Phi(X) &= \frac{\lambda^C}{\lambda^C + \lambda^U + \mu}\Phi(X-1) + \frac{\lambda^U}{\lambda^C + \lambda^U + \mu}(\delta_R + \Phi(X)), \\ \Phi(X) &= \frac{\lambda^C}{\lambda^C + \mu}\Phi(X-1) + \frac{\lambda^U}{\lambda^C + \mu}\delta_R. \end{aligned} \quad (15)$$

Thus, we can write the recursion as

$$\Phi(X) = \min\left\{\frac{\lambda^C + \lambda^U}{\lambda^C + \lambda^U + \mu}\Phi(X-1), \frac{\lambda^C}{\lambda^C + \mu}\Phi(X-1) + \frac{\lambda^U}{\lambda^C + \mu}\delta_R\right\} \quad (16)$$

Using (1), the expected total cost of the system after the camp inventory reaches zero,  $\Phi(0)$ , is:

$$\begin{aligned} \Phi(0) &= \frac{\lambda^C}{\lambda^C + \lambda^U + \mu} \times (\delta_D(\frac{\alpha}{\mu-\alpha}) + \Phi(0)) + \frac{\lambda^U}{\lambda^C + \lambda^U + \mu} \times (\delta_R + \Phi(0)) \\ \frac{\mu}{\lambda^C + \lambda^U + \mu}\Phi(0) &= \frac{\delta_D(\frac{\alpha}{\mu-\alpha})\lambda^C + \delta_R\lambda^U}{\lambda^C + \lambda^U + \mu} \\ \Phi(0) &= \frac{\delta_D(\frac{\alpha}{\mu-\alpha})\lambda^C + \delta_R\lambda^U}{\mu}. \end{aligned} \quad (17)$$

Given an initial allocation, we can use (16) and (17) to compute the total expected cost for each location at each cycle. We can also use the recursion to compute the point where the decision

switches from sharing to referral. After a camp decides to refer external refugees elsewhere at a given inventory level, it can be reasoned that no requests will be accepted below that inventory level. As each state includes the probability that the cycle will conclude prior to an additional demand occurrence, state expected costs can be seen as a decreasing function of inventory level, when the preferred option is to reject the request of an external refugee. The rate of decrease will slow down with increased inventory level, and at some point the cost will start to increase, where the camp will begin to satisfy external demand occurrences as well. We seek the threshold  $\Omega$ , where this transition occurs, which is essentially the global minimum of a unimodal convex function. To find the threshold, we use equation (14) for states where external demand occurrences are satisfied, and (15) for states where they are rejected. To summarize,  $\Omega$  should satisfy the two following conditions:

- External refugee demand should be referred elsewhere, when only  $\Omega$  units of aid are in inventory;
- External refugee demand should be accepted, when  $\Omega + 1$  units of aid are in inventory.

Therefore, for the threshold, the following inequalities must hold:

$$\frac{\lambda^C + \lambda^U}{\lambda^C + \lambda^U + \mu} \Phi(\Omega - 1) > \frac{\lambda^C}{\lambda^C + \mu} \Phi(\Omega - 1) + \frac{\lambda^U}{\lambda^C + \mu} \delta_R, \quad (18)$$

$$\frac{\lambda^C + \lambda^U}{\lambda^C + \lambda^U + \mu} \Phi(\Omega) < \frac{\lambda^C}{\lambda^C + \mu} \Phi(\Omega) + \frac{\lambda^U}{\lambda^C + \mu} \delta_R. \quad (19)$$

Inequality (18) represents the first case, whereas inequality (19) represents the second case. Using inequalities (18) and (19), lower and upper bounds for  $\Phi(\Omega - 1)$  can be derived. For the lower bound:

$$\begin{aligned} \frac{\lambda^C + \lambda^U}{\lambda^C + \lambda^U + \mu} \Phi(\Omega - 1) - \frac{\lambda^C}{\lambda^C + \mu} \Phi(\Omega - 1) &> \frac{\lambda^U}{\lambda^C + \mu} \delta_R, \\ \Phi(\Omega - 1) &> \frac{\lambda^C + \lambda^U + \mu}{\mu} \delta_R. \end{aligned} \quad (20)$$

For the upper bound:

$$\begin{aligned} \frac{\lambda^U}{\lambda^C + \mu} \delta_R &> \frac{\lambda^C + \lambda^U}{\lambda^C + \lambda^U + \mu} \Phi(\Omega) - \frac{\lambda^C}{\lambda^C + \mu} \Phi(\Omega), \\ \frac{\lambda^C + \lambda^U + \mu}{\mu} \delta_R &> \Phi(\Omega). \end{aligned}$$

As external refugee requests are refused when only  $\Omega$  items are on hand, we use (15) to obtain:

$$\begin{aligned} \frac{\lambda^C + \lambda^U + \mu}{\mu} \delta_R &> \frac{\lambda^C}{\lambda^C + \mu} \Phi(\Omega - 1) + \frac{\lambda^U}{\lambda^C + \mu} \delta_R, \\ \frac{(\lambda^C + \mu)^2}{\lambda^C \mu} \delta_R + \frac{\lambda^U}{\mu} \delta_R &> \Phi(\Omega - 1). \end{aligned} \quad (21)$$

Knowing that a camp with inventory level of  $X$  will reject external requests below that level, a closed-form equation for  $\Phi(X)$  is:

$$\begin{aligned}
\Phi(X) &= \frac{\lambda^C}{\lambda^C + \mu} \Phi(X-1) + \frac{\lambda^U}{\lambda^C + \mu} \delta_R \\
&= \frac{\lambda^C}{\lambda^C + \mu} \left( \frac{\lambda^C}{\lambda^C + \mu} \Phi(X-2) + \frac{\lambda^U}{\lambda^C + \mu} \delta_R \right) + \frac{\lambda^U}{\lambda^C + \mu} \delta_R \\
&= \left( \frac{\lambda^C}{\lambda^C + \mu} \right)^X \Phi(0) + \frac{\delta_R \lambda^U}{\lambda^C + \mu} \sum_{i=0}^{X-1} \left( \frac{\lambda^C}{\lambda^C + \mu} \right)^i \\
&= \left( \frac{\lambda^C}{\lambda^C + \mu} \right)^X \Phi(0) + \frac{\delta_R \lambda^U}{\lambda^C + \mu} \frac{1 - \left( \frac{\lambda^C}{\lambda^C + \mu} \right)^X}{1 - \left( \frac{\lambda^C}{\lambda^C + \mu} \right)}. \tag{22}
\end{aligned}$$

Using  $\Phi(0)$  from (17), equation (22) can be rearranged as:

$$\begin{aligned}
\Phi(X) &= \frac{\delta_D \left( \frac{\alpha}{\mu - \alpha} \right) \lambda^C + \delta_R \lambda^U}{\mu} \left( \frac{\lambda^C}{\lambda^C + \mu} \right)^X + \frac{\delta_R \lambda^U}{\mu} \left( 1 - \left( \frac{\lambda^C}{\lambda^C + \mu} \right)^X \right) \\
&= \frac{\delta_D \left( \frac{\alpha}{\mu - \alpha} \right) \lambda^C}{\mu} \left( \frac{\lambda^C}{\lambda^C + \mu} \right)^X + \frac{\delta_R \lambda^U}{\mu}. \tag{23}
\end{aligned}$$

Using (20), (21), and (23), the threshold  $\Omega$  can be computed as the smallest integer that satisfies:

$$\frac{\lambda^C + \mu}{\mu} \delta_R + \frac{\lambda^U}{\mu} \delta_R < \frac{\lambda^C}{\mu} \delta_D \left( \frac{\alpha}{\mu - \alpha} \right) \left( \frac{\lambda^C}{\lambda^C + \mu} \right)^{\Omega-1} + \frac{\lambda^U}{\mu} \delta_R < \frac{(\lambda^C + \mu)^2}{\lambda^C \mu} \delta_R + \frac{\lambda^U}{\mu} \delta_R,$$

which, after some algebra, yields the following condition:

$$\frac{\delta_R}{\delta_D \left( \frac{\alpha}{\mu - \alpha} \right)} < \left( \frac{\lambda^C}{\lambda^C + \mu} \right)^\Omega < \frac{\lambda^C + \mu}{\lambda^C} \times \frac{\delta_R}{\delta_D \left( \frac{\alpha}{\mu - \alpha} \right)}. \tag{24}$$

Under the necessary condition  $\frac{\delta_R}{\delta_D \left( \frac{\alpha}{\mu - \alpha} \right)} < 1$ , the threshold can be expressed as:

$$\Omega = \left\lceil \log \frac{\delta_R}{\delta_D \left( \frac{\alpha}{\mu - \alpha} \right)} / \log \frac{\lambda^C}{\lambda^C + \mu} \right\rceil. \tag{25}$$

### A.3 Cost Component Derivations

The expected costs of referral, deprivation, and holding are calculated with respect to the quantity of aid allocated and its relationship with the derived threshold. The expected total cost is also calculated by summing the individual cost components.

#### A.3.1 Expected Cost of Referral

**Case 1:**  $X > \Omega$ .

To calculate the expected cost of referral,  $E[C^R(X)]$ , it is necessary to derive the probability that the amount of aid consumed during a cycle is equal to the difference between the amount of aid allocated to the camp and its sharing threshold. With this probability, we multiply the

expected number of occurrences with rate  $\lambda^U$  in a duration with the rate of replenishment  $\mu$ , and the cost of referral per demand occurrence in the surrounding population.

$$E[C^R(X)] = \left( \frac{\lambda^C + \lambda^U}{\lambda^C + \lambda^U + \mu} \right)^{X-\Omega} \left( \frac{\lambda^U \delta_R}{\mu} \right). \quad (26)$$

**Case 2:**  $X \leq \Omega$ .

Knowing that the camp will not serve external demand requests, the expected cost of referral is:

$$E[C^R(X)] = \frac{\lambda^U \delta_R}{\mu}. \quad (27)$$

### A.3.2 Expected Deprivation Cost

**Case 1:**  $X > \Omega$ .

Following Lemma 1, the expected deprivation cost for a camp  $E[C^D(X)]$  becomes:

$$E[C^D(X)] = \delta_D \lambda^C \left( \frac{\lambda^C + \lambda^U}{\lambda^C + \lambda^U + \mu} \right)^{X-\Omega} \left( \frac{\lambda^C}{\lambda^C + \mu} \right)^\Omega \left( \frac{\alpha}{\mu - \alpha} \right). \quad (28)$$

Note that when the deprivation rate  $\alpha$  is exceedingly large, that is, when it exceeds the rate of replenishment  $\mu$ , the expected deprivation cost becomes negative, and deprivation becomes more attractive. For practical purposes, we only allow  $\alpha < \mu$ .

**Case 2:**  $X \leq \Omega$ .

$$E[C^D(X)] = \delta_D \lambda^C \left( \frac{\lambda^C}{\lambda^C + \mu} \right)^X \left( \frac{\alpha}{\mu - \alpha} \right). \quad (29)$$

### A.3.3 Expected Holding Cost

**Case 1:**  $X > \Omega$ .

The expected holding cost,  $E[C^H(X)]$ , is calculated as the product of the holding cost per unit time, the time between two events, and the amount of items in inventory between two event occurrences. Exponential distribution properties give the time between two events as  $\frac{1}{\lambda^C + \mu}$ , when a camp stops sharing its inventory with external refugees. Therefore, the expected holding cost of a single unit of aid in inventory is:

$$E[C^H(1)] = \frac{1}{\lambda^C + \mu} h. \quad (30)$$

The expected holding cost when there are two items in inventory is:

$$\begin{aligned} E[C^H(2)] &= 2 \times \frac{h}{\lambda^C + \mu} + \frac{\lambda^C}{\lambda^C + \mu} \times \frac{h}{\lambda^C + \mu} \\ &= \frac{h}{\lambda^C + \mu} \left( 2 + \frac{\lambda^C}{\lambda^C + \mu} \right). \end{aligned} \quad (31)$$

Generalizing, the expected holding cost for  $S$  items in inventory after the camp begins referring external requests is:

$$E[C^H(S)] = S \times \frac{h}{\lambda^C + \mu} + \frac{\lambda^C}{\lambda^C + \mu} \times E[C^H(S-1)]. \quad (32)$$

Therefore, the expected holding cost when there are  $\Omega$  units in inventory is:

$$\begin{aligned} E[C^H(\Omega)] &= \frac{h}{\lambda^C + \mu} \left( \sum_{i=0}^{\Omega-1} \left( \frac{\lambda^C}{\lambda^C + \mu} \right)^{\Omega-1-i} (i+1) \right) \\ &= \frac{h}{\mu^2} \left( \lambda^C \left( \left( \frac{\lambda^C}{\lambda^C + \mu} \right)^\Omega - 1 \right) + \mu\Omega \right). \end{aligned} \quad (33)$$

Beyond the sharing threshold  $\Omega$ , the rate  $\lambda^U$  is observed in addition to rates  $\lambda^C$  and  $\mu$ . The corresponding time between two events is  $\frac{1}{\lambda^C + \lambda^U + \mu}$ , and the expected holding cost calculation is adjusted accordingly. For inventory levels above the threshold, the expected holding cost is:

$$E[C^H(S)] = S \times \frac{h}{\lambda^C + \lambda^U + \mu} + \frac{\lambda^C + \lambda^U}{\lambda^C + \lambda^U + \mu} \times E[C^H(S-1)]. \quad (34)$$

Using the definition in equation (34), expected inventory holding costs for  $\Omega + 1$  and  $\Omega + 2$  are:

$$\begin{aligned} E[C^H(\Omega + 1)] &= \frac{h}{\lambda^C + \lambda^U + \mu} (\Omega + 1) + \frac{\lambda^C + \lambda^U}{\lambda^C + \lambda^U + \mu} E[C^H(\Omega)], \\ E[C^H(\Omega + 2)] &= \frac{h}{\lambda^C + \lambda^U + \mu} (\Omega + 2) + \frac{\lambda^C + \lambda^U}{\lambda^C + \lambda^U + \mu} E[C^H(\Omega + 1)]. \end{aligned}$$

A generalized form of expected holding cost for  $X$  items in inventory when  $X > \Omega$  is:

$$E[C^H(X)] = \frac{h}{\lambda^C + \lambda^U + \mu} \left[ \sum_{i=0}^{X-\Omega-1} \left( \frac{\lambda^C + \lambda^U}{\lambda^C + \lambda^U + \mu} \right)^{X-\Omega-1-i} (\Omega + 1 + i) \right] + \left( \frac{\lambda^C + \lambda^U}{\lambda^C + \lambda^U + \mu} \right)^{X-\Omega} E[C^H(\Omega)]. \quad (35)$$

After simplification, the expected holding cost for  $X$  items in inventory can be found as:

$$\begin{aligned} E[C^H(X)] &= \frac{h}{\mu^2} \left[ \left( 1 - \left( \frac{\lambda^C + \lambda^U}{\lambda^C + \lambda^U + \mu} \right)^{X-\Omega} \right) (\mu\Omega - \lambda^C - \lambda^U) + \mu(X - \Omega), \right. \\ &\quad \left. + \left( \frac{\lambda^C + \lambda^U}{\lambda^C + \lambda^U + \mu} \right)^{X-\Omega} \left( \lambda^C \left( \left( \frac{\lambda^C}{\lambda^C + \mu} \right)^\Omega - 1 \right) + \mu\Omega \right) \right]. \end{aligned} \quad (36)$$

**Case 2:  $X \leq \Omega$ .**

Using equation (33), expected total holding cost of the camp when initial inventory is  $X$  items can be calculated as:

$$\begin{aligned} E[C^H(X)] &= \frac{h}{\lambda^C + \mu} \left( \sum_{i=0}^{X-1} \left( \frac{\lambda^C}{\lambda^C + \mu} \right)^{X-1-i} (i+1) \right), \\ &= \frac{h}{\mu^2} \left( \lambda^C \left( \left( \frac{\lambda^C}{\lambda^C + \mu} \right)^X - 1 \right) + \mu X \right). \end{aligned} \quad (37)$$

### A.3.4 Expected Total Cost for a Camp: Sum of Referral, Deprivation, Holding

**Case 1:**  $X > \Omega$ .

Using equations (36), (28), and (26), expected total cost of the system can be calculated as follows:

$$E[C^T(X)] = \left( \frac{\lambda^C + \lambda^U}{\lambda^C + \lambda^U + \mu} \right)^{X-\Omega} \left( \frac{\lambda^U \delta_R}{\mu} \right) + \delta_D \lambda^C \left( \frac{\lambda^C + \lambda^U}{\lambda^C + \lambda^U + \mu} \right)^{X-\Omega} \left( \frac{\lambda^C}{\lambda^C + \mu} \right)^\Omega \left( \frac{\alpha}{\mu - \alpha} \right) \\ + \frac{h}{\mu^2} \left[ \left( 1 - \left( \frac{\lambda^C + \lambda^U}{\lambda^C + \lambda^U + \mu} \right)^{X-\Omega} \right) (\mu\Omega - \lambda^C - \lambda^U) + \mu(X - \Omega) + \left( \frac{\lambda^C + \lambda^U}{\lambda^C + \lambda^U + \mu} \right)^{X-\Omega} \right], \\ \times \left( \lambda^C \left( \left( \frac{\lambda^C}{\lambda^C + \mu} \right)^\Omega - 1 \right) + \mu\Omega \right) \quad (38)$$

$$E[C^T(X)] = \left( \frac{\lambda^C + \lambda^U}{\lambda^C + \lambda^U + \mu} \right)^X \left( \frac{\lambda^C + \lambda^U + \mu}{\lambda^C + \lambda^U} \right)^\Omega \left[ \lambda^U \left( \frac{h}{\mu^2} + \frac{\delta_R}{\mu} \right) + \lambda^C \left( \frac{\lambda^C}{\lambda^C + \mu} \right)^\Omega \left( \frac{h}{\mu^2} + \delta_D \left( \frac{\alpha}{\mu - \alpha} \right) \right) \right] \\ + \frac{hX}{\mu} + \frac{h}{\mu^2} (-\lambda^C - \lambda^U). \quad (39)$$

**Case 2:**  $X \leq \Omega$ .

Expected total cost of the system when  $X \leq \Omega$  can be calculated From equations (37), (29), and (27):

$$E[C^T(X)] = \frac{\lambda^U \delta_R}{\mu} + \delta_D \lambda^C \left( \frac{\lambda^C}{\lambda^C + \mu} \right)^X \left( \frac{\alpha}{\mu - \alpha} \right) + \frac{h}{\mu^2} \left( \lambda^C \left( \left( \frac{\lambda^C}{\lambda^C + \mu} \right)^X - 1 \right) + \mu X \right), \quad (40)$$

$$E[C^T(X)] = \left( \delta_D \lambda^C \left( \frac{\alpha}{\mu - \alpha} \right) + \frac{h\lambda^C}{\mu^2} \right) \left( \frac{\lambda^C}{\lambda^C + \mu} \right)^X + \frac{hX}{\mu} + \frac{\lambda^U \delta_R}{\mu} - \frac{h\lambda^C}{\mu^2}. \quad (41)$$

Expected total cost functions defined for the two cases above in (39) and (41) can be written together as

$$E[C^T(X_i)] = \gamma_1(\cdot) \gamma_2(\cdot)^{X_i} + hX_i/\mu + \gamma_3(\cdot) \quad (42)$$

that uses the three components below:

$$\gamma_1(X_i, \Omega_i, h, \lambda_i^C, \lambda_i^U, \mu, \delta_R, \delta_D, \alpha) = \begin{cases} \left( \frac{\lambda_i^C + \lambda_i^U + \mu}{\lambda_i^C + \lambda_i^U} \right)^{\Omega_i} \left[ \lambda_i^U \left( \frac{h}{\mu^2} + \frac{\delta_R}{\mu} \right) \right. \\ \left. + \lambda_i^C \left( \frac{\lambda_i^C}{\lambda_i^C + \mu} \right)^{\Omega_i} \left( \frac{h}{\mu^2} + \delta_D \left( \frac{\alpha}{\mu - \alpha} \right) \right) \right] & \text{if } X_i > \Omega_i, \\ \left( \delta_D \lambda_i^C \left( \frac{\alpha}{\mu - \alpha} \right) + \frac{h\lambda_i^C}{\mu^2} \right) & \text{otherwise;} \end{cases} \quad (43)$$

$$\gamma_2(X_i, \Omega_i, \lambda_i^C, \lambda_i^U, \mu) = \begin{cases} \frac{\lambda_i^C + \lambda_i^U}{\lambda_i^C + \lambda_i^U + \mu} & \text{if } X_i > \Omega_i, \\ \frac{\lambda_i^C}{\lambda_i^C + \mu} & \text{otherwise;} \end{cases} \quad (44)$$

$$\gamma_3(X_i, \Omega_i, h, \lambda_i^C, \lambda_i^U, \mu, \delta_R) = \begin{cases} \frac{h}{\mu^2} (-\lambda_i^C - \lambda_i^U) & \text{if } X_i > \Omega_i, \\ \frac{\lambda_i^U \delta_R}{\mu} - \frac{h\lambda_i^C}{\mu^2} & \text{otherwise.} \end{cases} \quad (45)$$

#### A.4 Proof of Proposition 1

The expected total cost  $E[C^T(X_i)]$  for camp  $i$  when  $X_i > \Omega_i$  is:

$$\begin{aligned}
E[C^T(X_i)] &= \left( \frac{\lambda^C + \lambda^U}{\lambda^C + \lambda^U + \mu} \right)^{X_i} \left( \frac{\lambda^C + \lambda^U + \mu}{\lambda^C + \lambda^U} \right)^{\Omega_i} \left[ \lambda^U \left( \frac{h}{\mu^2} + \frac{\delta_R}{\mu} \right) + \lambda^C \left( \frac{\lambda^C}{\lambda^C + \mu} \right)^{\Omega_i} \right. \\
&\quad \left. \times \left( \frac{h}{\mu^2} + \delta_D \left( \frac{\alpha}{\mu - \alpha} \right) \right) \right] + \frac{hX_i}{\mu} + \frac{h}{\mu^2} (-\lambda^C - \lambda^U) \\
&= \left( \frac{\lambda^C + \lambda^U}{\lambda^C + \lambda^U + \mu} \right)^{X_i - \Omega_i} \left[ \frac{h\lambda^U}{\mu^2} + \frac{\lambda^U \delta_R}{\mu} + \left( \frac{h\lambda^C}{\mu^2} + \delta_D \lambda^C \left( \frac{\alpha}{\mu - \alpha} \right) \right) \left( \frac{\lambda^C}{\lambda^C + \mu} \right)^{\Omega_i} \right] \\
&\quad + \frac{hX_i}{\mu} - \frac{h\lambda^C}{\mu^2} - \frac{h\lambda^U}{\mu^2} \\
&= \left( \frac{\lambda^C + \lambda^U}{\lambda^C + \lambda^U + \mu} \right)^{X_i - \Omega_i} \left[ \left( \delta_D \lambda^C \left( \frac{\alpha}{\mu - \alpha} \right) + \frac{h\lambda^C}{\mu^2} \right) \left( \frac{\lambda^C}{\lambda^C + \mu} \right)^{\Omega_i} + \frac{\lambda^U \delta_R}{\mu} \right] \\
&\quad + \frac{hX_i}{\mu} - \frac{h\lambda^C}{\mu^2}.
\end{aligned}$$

If the allocation satisfies  $X_i \leq \Omega_i$ , then the expected total cost for camp  $i$  is:

$$E[C^T(X_i)] = \left( \delta_D \lambda^C \left( \frac{\alpha}{\mu - \alpha} \right) + \frac{h\lambda^C}{\mu^2} \right) \left( \frac{\lambda^C}{\lambda^C + \mu} \right)^{X_i} + \frac{hX_i}{\mu} + \frac{\lambda^U \delta_R}{\mu} - \frac{h\lambda^C}{\mu^2}.$$

It can be seen that  $C^T(\Omega_i)$  for both of the cases above are equal, as follows:

$$E[C^T(\Omega_i)] = \left( \delta_D \lambda^C \left( \frac{\alpha}{\mu - \alpha} \right) + \frac{h\lambda^C}{\mu^2} \right) \left( \frac{\lambda^C}{\lambda^C + \mu} \right)^{\Omega_i} + \frac{h\Omega_i}{\mu} + \frac{\lambda^U \delta_R}{\mu} - \frac{h\lambda^C}{\mu^2}.$$

## B Optimal Allocations Under Known Allocation-Threshold Relationships

When the order up to level for each camp is a priori known to be either above, equal to, or below the sharing threshold, we show how to analytically derive optimal levels.

Let  $\Gamma_i$  denote the given set of restrictions on the order up to level for camp  $i$ , where  $\Gamma_i$  is a closed subset of either  $X_i \leq \Omega_i$  or  $X_i \geq \Omega_i$ . When  $X_i \in \Gamma_i, \forall i \in \{1, \dots, N\}$ , Proposition 1 ensures that component functions are independent from the  $X_i$  and  $\Omega_i$  relationships.

$$\min_{\mathbf{X} \in \mathbf{\Gamma}} E[C^T(\mathbf{X})] = \sum_{i=1}^N \gamma_1(h, \lambda_i^C, \lambda_i^U, \mu, \delta_R, \delta_D, \alpha) \left[ \gamma_2(\lambda_i^C, \lambda_i^U, \mu) \right]^{X_i} + \gamma_3(h, \lambda_i^C, \lambda_i^U, \mu, \delta_R) + h\mathcal{S}/\mu \quad (46a)$$

$$\text{subject to } \sum_{i=1}^N (X_i - I_i) \leq \mathcal{S}. \quad (46b)$$

Note that the component functions are no longer functions of  $X_i$  and  $\Omega_i$ , as sets  $\mathbf{\Gamma}$  a priori indicate boundary conditions in the piecewise cost functions as per Theorem 2. Hence, the functions only require the parameters specified in formulation (46).

The Lagrangian dual of formulation (46) can be written as follows:

$$\max_{\pi \geq 0} \Theta(\pi) = \min_{\mathbf{X} \in \mathbf{\Gamma}} \sum_{i=1}^N \gamma_1(h, \lambda_i^C, \lambda_i^U, \mu, \delta_R, \delta_D, \alpha) \left[ \gamma_2(\lambda_i^C, \lambda_i^U, \mu) \right]^{X_i} + \gamma_3(h, \lambda_i^C, \lambda_i^U, \mu, \delta_R) + h\mathcal{S}/\mu + \pi \left( \sum_{i=1}^N (X_i - I_i) - \mathcal{S} \right). \quad (47)$$

First, if there exists a feasible  $\mathbf{X}$  for the primal problem and a feasible  $\pi$  to the dual problem such that  $C^T(\mathbf{X}) = \Theta(\pi)$ , then  $\mathbf{X}$  is the optimal solution, and complementary slackness holds (Bazaraa et al., 2013). There are two cases. In the first, the total allocation is such that excess inventory exists in the distribution center at optimality, so that there is slack in the system, and  $\pi = 0$ . In the second, the entire supply  $\mathcal{S}$  is distributed to camps in the system, so that constraint (46b) is binding at optimality, i.e.,  $\sum_{i=1}^N (X_i - I_i) = \mathcal{S}$ . Consequently,  $\pi$  can be increased, while primal and dual objectives are equal. Thus, in this case we seek to determine for a given  $\pi$ , what is the optimal  $\mathbf{X}$  that consumes the central supply  $\mathcal{S}$ .

For both cases, optimality conditions can be derived using the Jacobian for the objective function in (47) for a given  $\pi$ , which we denote as  $\Phi(\mathbf{X}, \pi)$ . The  $i^{\text{th}}$  function in the Jacobian is:

$$\frac{\partial \Phi(\mathbf{X}, \pi)}{\partial X_i} = \gamma_1(h, \lambda_i^C, \lambda_i^U, \mu, \delta_R, \delta_D, \alpha) \ln \gamma_2(\lambda_i^C, \lambda_i^U, \mu) \gamma_2(\lambda_i^C, \lambda_i^U, \mu)^{X_i} + \pi. \quad (48)$$

This leads us to the following Lemma:

**Lemma 2.** *A solution is suboptimal if there is excess inventory in the distribution center and there exists a camp that can attain a higher allocation level.*

*Proof.* The natural logarithm of a positive number less than 1 implies that the first term is always negative. Suppose that  $\sum_{i=1}^N (X_i - I_i) < \mathcal{S}$ , that is, excess inventory exists in the distribution

center at optimality; consequently  $\pi = 0$ . In this case, the objective function always decreases as  $\mathbf{X}$  increases. Then the optimal action is to allocate as much as possible for each camp, within the given restrictions.  $\square$

**Theorem 3.** *In the absence of other additional restrictions to order up to levels, all supplies are allocated at optimality and no excess inventory exists in the distribution center.*

*Proof.* The proof immediately follows from Lemma 2.  $\square$

Theorem 3 shows that, if feasible, the entirety of the supply  $\mathcal{S}$  will be allocated at optimality, and constraint (46b) is binding. The  $i^{\text{th}}$  diagonal entry of the Hessian matrix is:

$$\frac{\partial^2 \Phi(\mathbf{X}, \pi)}{\partial X_i^2} = \gamma_1(h, \lambda_i^C, \lambda_i^U, \mu, \delta_R, \delta_D, \alpha) (\ln \gamma_2(\lambda_i^C, \lambda_i^U, \mu))^2 \gamma_2(\lambda_i^C, \lambda_i^U, \mu)^{X_i}. \quad (49)$$

Expression (49) is positive for all  $i$  and all off-diagonal entries of the matrix are zero, thus the Hessian is positive definite and  $\Phi(\mathbf{X}, \pi)$  is strictly convex on  $\mathbf{X}$ .

Let  $\mathbf{X}^0$  be a feasible *critical point*, that is,  $\mathbf{X}^0 \in \mathbf{\Gamma}$  and  $\frac{\partial \Phi(\mathbf{X}^0, \pi^0)}{\partial X_i} = 0$  for all  $i$ . Then solving the following system of equations will yield a global optimum.

$$\gamma_1(h, \lambda_i^C, \lambda_i^U, \mu, \delta_R, \delta_D, \alpha) \ln \gamma_2(\lambda_i^C, \lambda_i^U, \mu) \gamma_2(\lambda_i^C, \lambda_i^U, \mu)^{X_i^0} + \pi^0 = 0, \quad i = 1, \dots, N \quad (50)$$

$$\sum_{i=1}^N X_i^0 = \mathcal{S} + \sum_{i=1}^N I_i. \quad (51)$$

The first  $N$  equations can be rewritten as

$$\pi^0 = -\gamma_1(h, \lambda_i^C, \lambda_i^U, \mu, \delta_R, \delta_D, \alpha) \ln \gamma_2(\lambda_i^C, \lambda_i^U, \mu) \gamma_2(\lambda_i^C, \lambda_i^U, \mu)^{X_i^0}, \quad i = 1, \dots, N,$$

where the logarithm of both sides is obtained as

$$\ln \pi^0 = \ln \gamma_1(h, \lambda_i^C, \lambda_i^U, \mu, \delta_R, \delta_D, \alpha) + \ln(-\ln \gamma_2(\lambda_i^C, \lambda_i^U, \mu)) + \ln \gamma_2(\lambda_i^C, \lambda_i^U, \mu)^{X_i^0}, \quad i = 1, \dots, N. \quad (52)$$

The logarithm of the first  $N$  equations in (52), together with the last equation in (51), provide us with  $N + 1$  linearly independent equations and  $N + 1$  unknowns:

$$\ln \gamma_2(\lambda_i^C, \lambda_i^U, \mu)^{X_i^0} - \ln \pi^0 = -\ln \gamma_1(h, \lambda_i^C, \lambda_i^U, \mu, \delta_R, \delta_D, \alpha) - \ln(-\ln \gamma_2(\lambda_i^C, \lambda_i^U, \mu)) \quad i = 1, \dots, N, \quad (53)$$

$$\sum_{i=1}^N X_i^0 = \mathcal{S} + \sum_{i=1}^N I_i. \quad (54)$$

Then, we can substitute  $\ln \pi^0$  with a new nonnegative variable ( $\pi^0$ ) and the closed-form solution for  $\mathbf{X}^0, \pi^0$  can be obtained as

$$\mathbf{X}^0, \pi^0 = A^{-1}b, \quad (55)$$

where

$$A = \begin{bmatrix} \ln \gamma_2(\lambda_1^C, \lambda_1^U, \mu) & 0 & \cdots & 0 & -1 \\ 0 & \ln \gamma_2(\lambda_2^C, \lambda_2^U, \mu) & \cdots & 0 & -1 \\ \vdots & \vdots & \ddots & \vdots & \vdots \\ 0 & 0 & \cdots & \ln \gamma_2(\lambda_N^C, \lambda_N^U, \mu) & -1 \\ 1 & 1 & \cdots & 1 & 0 \end{bmatrix}, \quad (56)$$

and

$$b = \begin{bmatrix} -\ln \gamma_1(h, \lambda_1^C, \lambda_1^U, \mu, \delta_R, \delta_D, \alpha) - \ln(-\ln \gamma_2(\lambda_1^C, \lambda_1^U, \mu)) \\ -\ln \gamma_1(h, \lambda_2^C, \lambda_2^U, \mu, \delta_R, \delta_D, \alpha) - \ln(-\ln \gamma_2(\lambda_2^C, \lambda_2^U, \mu)) \\ \vdots \\ -\ln \gamma_1(h, \lambda_N^C, \lambda_N^U, \mu, \delta_R, \delta_D, \alpha) - \ln(-\ln \gamma_2(\lambda_N^C, \lambda_N^U, \mu)) \\ \mathcal{S} + \sum_{i=1}^N I_i \end{bmatrix}. \quad (57)$$

We back-substitute the new non-negative  $\pi^0$  variable in the solution of system (56)–(57) to obtain the optimal  $\pi^0$  value – which represents the marginal value of one unit of aid, and because  $\pi^0 = e^{\pi^0}$ , is guaranteed to be nonnegative.

Such a closed-form derivation is particularly noteworthy in the context of an unconstrained environment and abundance of supply to be distributed, where each camp will reasonably exceed its respective threshold, and so the result in (55) provides the optimal order up to levels. Moreover, the optimal order up to levels for each camp exceeds the threshold around the same total supply quantity. That said, the initial feasibility assertion for the critical point (i.e.,  $\mathbf{X}^0 \in \mathbf{\Gamma}$ ) is not guaranteed. As the critical point might be outside the given boundaries, a more general solution approach is presented in § 4.4.2.

## C Sensitivity of Costs Against Allocation Decisions, Replenishment Distribution, and Problem Parameters

We conduct an extensive computational sensitivity analysis to evaluate the performance of our derived optimal sharing thresholds and allocation levels. As detailed in Section 4.2, our sharing threshold derivations rely upon the assumption of exponentially distributed replenishment cycle durations. Our sensitivity analysis varies five key parameters directly involved in our optimal threshold derivations and the corresponding optimal levels of allocation. For each fixed level of these parameters (run), we evaluate the performance of the corresponding optimal sharing thresholds and resulting allocations by simulating replenishment cycle durations from three distinct distributions (exponential, lognormal, and uniform), and observing the behavior of the total cost.

We vary the following five parameters:

- Expected replenishment duration of 6, 9, and 12 months<sup>8</sup>
- Deprivation coefficient,  $\delta_D \in \{20, 30, 40, 50\}$
- Deprivation rate,  $\alpha \in \{0.25, 0.5, 0.75\}$
- Referral cost for unmet external demand,  $\delta_R \in \{1, 2, 3\}$
- Allocable supply from central decision-maker to refugee camps in refugee camp system,  $S \in \{ \text{Low, Medium, High} \}$ , as detailed in Table 7.

	Supply Value
<b>Low</b>	$\left( \sum_{i=1}^N \lambda_i^C + \frac{1}{2} \cdot \sum_{i=1}^N \lambda_i^U \right) / \mu$
<b>Medium</b>	$\left( \sum_{i=1}^N \lambda_i^C + \frac{2}{3} \cdot \sum_{i=1}^N \lambda_i^U \right) / \mu$
<b>High</b>	$\left( \sum_{i=1}^N \lambda_i^C + \sum_{i=1}^N \lambda_i^U \right) / \mu$

Table 7: Considered levels of allocable supply from central decision-maker to refugee camps in sensitivity analysis.

From all  $3^3 \times 4 = 108$  combinations of the first four parameters, we maintain all but a single combination from our sensitivity analysis:  $\{\mu = 2, \delta_D = 20, \alpha = 0.25, \delta_R = 3\}$ , as it generates negative sharing thresholds and thus does not satisfy the stated conditions required for our derivations to hold in the manuscript, namely violating Remark 2. This process results in a total of  $108 - 1 = 107$  combinations of levels for the first four parameters, and when spread across 3 levels of allocable supply  $S$ , generates 321 unique runs. For each run, we compute the optimal threshold levels as per Theorem 1, and solve optimization model (9) to compute the optimal order up to levels.

While our results in Theorem 1 and formulation (9) rely on properties of the exponential distribution, we aim to show how different distributions and various parameters affect cost components,

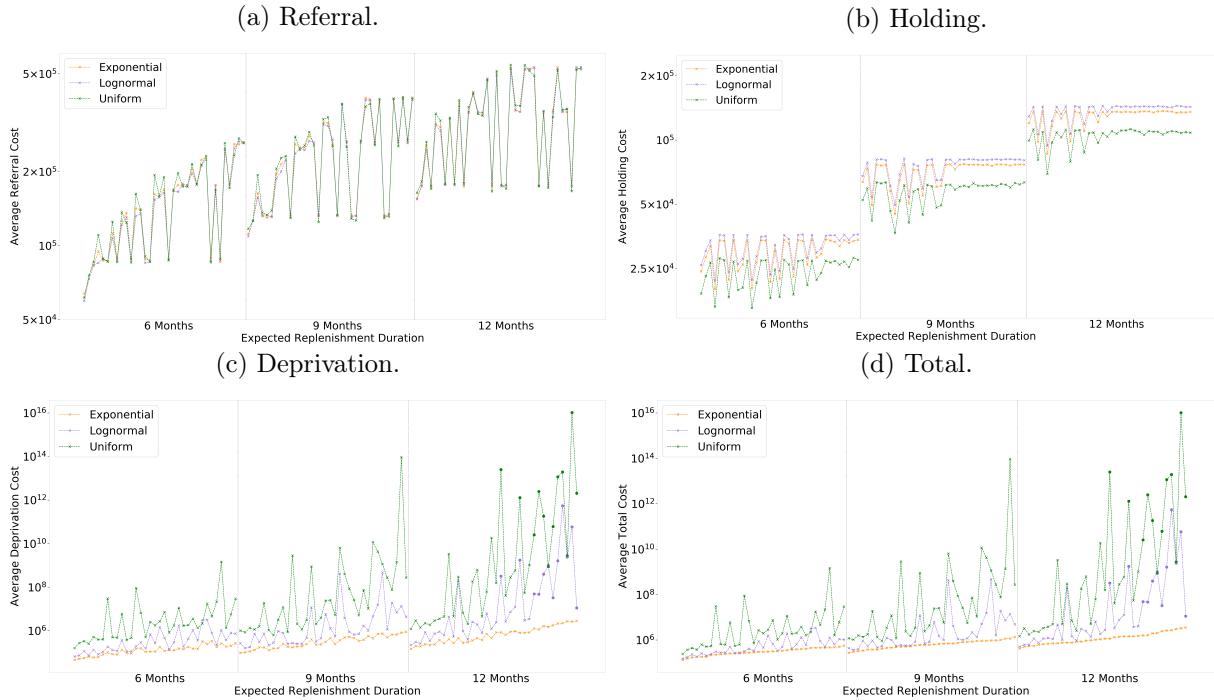
<sup>8</sup>The associated exponential distribution has mean  $\{1, 4/3, 2\}$  and variance  $\{1, 16/9, 4\}$ , with other distributions adjusted accordingly.

derived optimal thresholds, and related optimal order up to levels (allocations) performance. Accordingly, we now detail our evaluation through conducting extensive simulations on each of the 321 runs over 1,000 replicates of stochastically generated demand and replenishment<sup>9</sup>.

For demand events, we generate Poisson arrivals from internal and external populations for each camp according to demand rates described in Section 5. For replenishment events, we consider ten replenishment cycles per replicate using exponential, lognormal, and uniform distributions. As our derivations are based on an exponential distribution with mean  $1/\mu$  and variance  $1/\mu^2$ , we set the parameters for lognormal to  $\mu = -\ln(\sqrt{2}\mu)$  and  $\sigma = \sqrt{\ln(2)}$  to provide the same mean and variance. For the uniform distribution, we first generate one exponential random variable with rate  $10/\mu$  for the entire simulation horizon of ten cycles, and uniformly generate nine additional points within this horizon for a total of ten interarrivals.

For each replicate, we compute the cost of each camp separately according to the generated arrivals, replenishments, and cost parameters. Considering each demand event in chronological order, we decrease our inventory by one if the demand is internal and we have a positive inventory level, or if the demand is external and we have an inventory level above the threshold. The holding costs are updated based on the current inventory level and the time elapsed since the last demand observed. For an internal demand event, if the inventory is depleted, we compute the deprivation cost to be charged until the next replenishment. In external demand cases, the unsatisfied demand cases incur a referral cost.

Figure 8: Comparing cost components under three simulated replenishment distributions for allocable supply equal to expected demand of *internal plus two-thirds of external*.



<sup>9</sup>The Java code that performs these simulations and reports the costs for each replicate, as well as the Python code that analyzes the simulation results, are both available at <https://users.wpi.edu/~atrapp/tools-and-software.htm>

Figure 9: Comparing total costs for 2 allocable supply levels across 3 replenishment distributions.

(a) Expected demand of *internal plus half of external* (b) Expected demand of *internal plus full external*

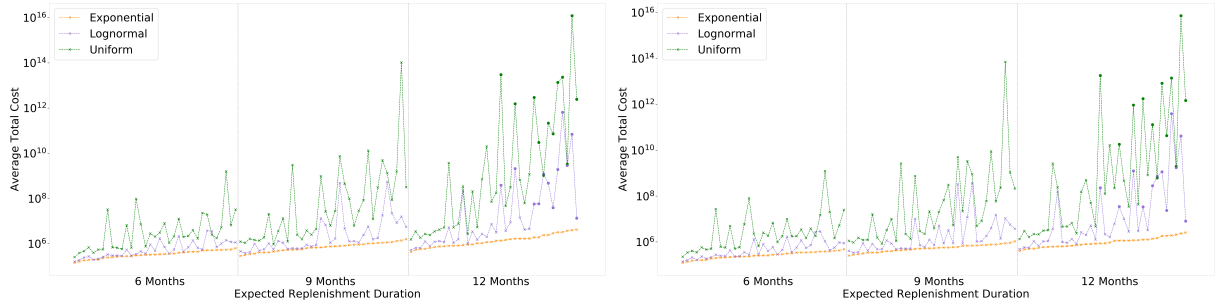
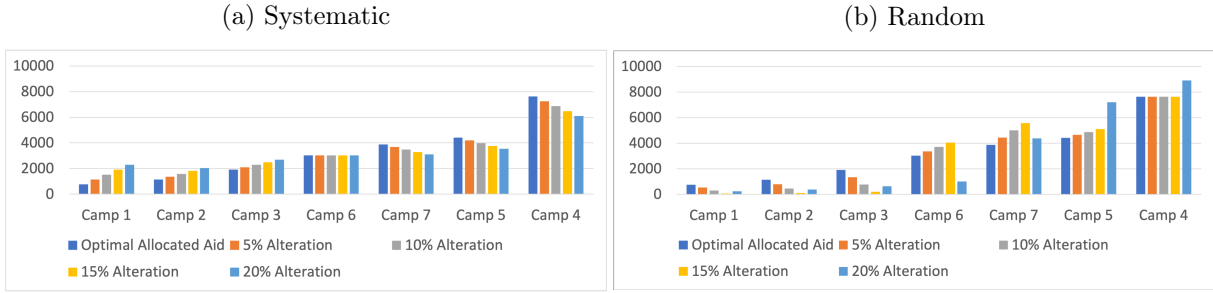


Figure 8 shows referral, holding, deprivation, and total costs for each of the 321 runs, averaged over 1,000 replicates, conducted under three different distributions for replenishment cycles when the total allocable supply  $S$  is equal to the expected demand of *internal plus two-thirds of external*. We observe that the referral and holding costs in Figures 8a and 8b are similar, with no significant difference in behavior or magnitude across different distributions and parameters. On the other hand, deprivation costs, which by nature are very sensitive to the uncertain replenishment lengths, vary depending on the problem parameters and the replenishment distribution type. We observe that for longer replenishment cycles and higher deprivation rates, there are increases in both the total cost as well as the sensitivity against the distribution type. This leads to a separation in Figure 8c, where we highlight the runs with the longest replenishment cycle and largest deprivation rate. We observe in Figure 9 that the total allocable supply has minimal effect on the separation of costs for different distributions. In some regards, these separations are not surprising because the random variables generated for replenishment cycles are aligned with our theoretical results only in terms of the first and second moment. Even so, allocation decisions are more critical compared to under/overestimation of costs, thus we next evaluate the sensitivity of our findings by purposefully deviating from the optimal order up to level allocations.

We alter the optimal order up to level allocations from the solution of formulation (9) in two ways: (i) *systematic* alteration by moving a small percentage of the allocated inventory from half of the camps to the other half, and (ii) *random* alteration by moving a small percentage of the allocated inventory among camps randomly. For systematic alteration, we use optimal allocated inventory levels and move a percentage of the  $n^{\text{th}}$  largest inventory to the  $n^{\text{th}}$  smallest inventory, with  $n$  varying from one camp to up to half the number of camps. In random alteration, we first compute a fraction of the total allocated inventory to be moved. Next, we flag at least half of the camps as givers, while ensuring they have enough inventory to satisfy the quantity to be moved. Depending on their inventory level and quantity to be moved, we compute a percentage that each giver should provide. Finally, we randomly chose a receiver from the remaining camps and transfer the required quantities from each giver camp Figure 10 depicts a small example comparing allocations according to systematic and random alteration. While systematic transfers clearly cause divergence from the optimal allocation, random alteration can be observed to go in any direction. If small camps are randomly chosen to give, for increased alteration percentage the number of camps that are required to give also increase. This, together with a large camp randomly being a receiver, may lead to an unexpected distribution of resources and some camps exceeding their thresholds, and consequently drastic changes in the flow of simulations with positive or negative outcomes.

Figure 10: Demonstrating Systematic and Random Alteration.

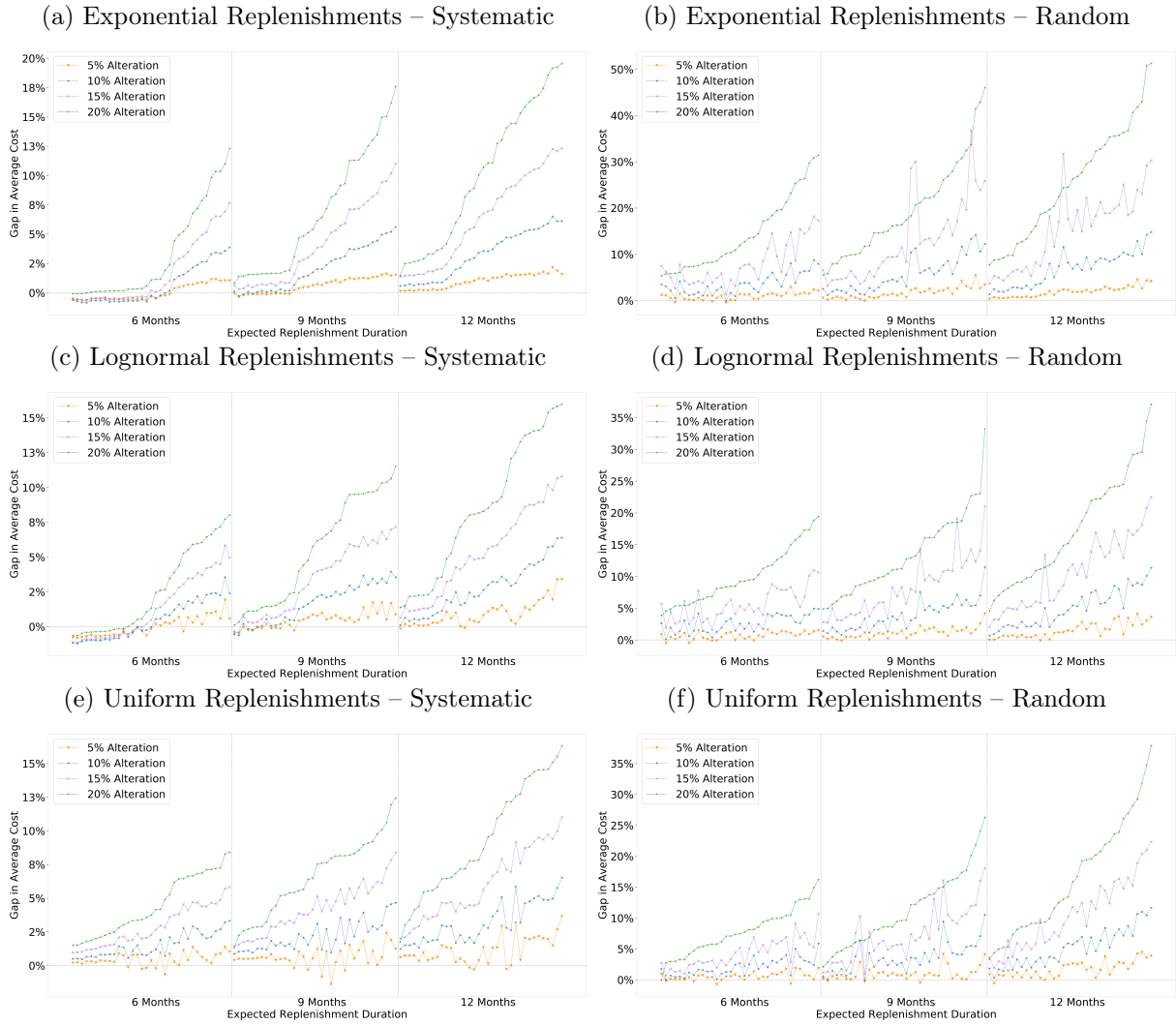


We ensure the simulations feature the same randomly generated replenishment cycles to alleviate some of the effects of randomness. On the whole we would expect to see our optimal allocations provide better cost performance compared to systematic and randomly altered solutions.

We show the gap between the optimal versus altered allocations in Figure 11. We show systematic and random alteration results for exponential, lognormal, and uniform replenishment cycles with a total allocable supply equal to the expected demand of *internal plus two thirds of the external*. The results of each run is again averaged over 1,000 replicates. These results show:

- Optimal allocation is better than altered allocations in a large majority of runs across all distributions;
- The deterioration of altered allocations is more exaggerated when replenishment cycles are longer and deprivation rates are higher;
- The runs where altered allocations may exhibit slightly better simulated performance than optimal allocations even under exponential distribution, are the cases where replenishments are frequent and deprivation rate  $\alpha$  tends to be low, which is consistent across all distributions.

Figure 11: Effect of altering optimal allocations under different replenishment distributions for allocable supply equal to expected demand of *internal plus two-thirds of external*.



In Table 8 we summarize these results for the three allocable supply levels and report the fraction of runs where optimal allocations outperform altered allocations in terms of the total cost objective averaged over all 1,000 simulated replicates. We observe that the results are similar across distributions, and although we use exponential replenishments for our derivations, the optimal allocation performs even better under the other two distributions. Not only is this unexpected, but also demonstrates the value of our analytical results from the viewpoint of practice.

When these changes are viewed more holistically, we observe a number of important points. First, it should be noted that these are for a limited number of replications (1,000); after a sufficient number of experiments, the optimal allocation should theoretically perform better than altered allocation under all other solutions for exponential distribution. Second, lower values appear for lower percent levels of alteration, and when the percent levels of alteration are higher, optimal allocation clearly trends to outperforming altered allocation nearly 100% of the time. This suggests that these lower values are simply the result of the influence of randomness. Third, and perhaps most important, the magnitude of the outperformance must also be considered to draw a proper conclusion when comparing optimal versus altered allocations. For instance,

Table 8: Percent of runs for which optimal allocation outperforms (averaged) altered allocation.

Supply	Alteration Type	% Difference with Optimal Allocations	Exponential	Lognormal	Uniform
Low	Random	5%	96.3	89.7	86.0
		10%	99.1	99.1	100.0
		15%	100.0	100.0	100.0
		20%	100.0	100.0	99.1
	Systematic	5%	74.8	71.0	86.9
		10%	82.2	81.3	100.0
		15%	86.9	86.0	100.0
		20%	89.7	89.7	100.0
Medium	Random	5%	94.4	92.5	87.9
		10%	99.1	100.0	99.1
		15%	100.0	100.0	100.0
		20%	100.0	100.0	99.1
	Systematic	5%	67.3	70.1	87.9
		10%	77.6	78.5	100.0
		15%	84.1	83.2	100.0
		20%	96.3	88.8	100.0
High	Random	5%	96.3	98.1	88.8
		10%	100.0	100.0	96.3
		15%	100.0	100.0	99.1
		20%	100.0	100.0	100.0
	Systematic	5%	56.1	70.1	96.3
		10%	73.8	84.1	100.0
		15%	79.4	88.8	100.0
		20%	100.0	99.1	100.0

Table 9: Averaged Percent of Positive, and Negative, Gaps of Altered Allocations With Respect to the Optimal Allocation.

Supply	Alteration Type	% Difference with Optimal Allocations	Exponential		Lognormal		Uniform	
			Average Negative Percentage Gap	Average Positive Percentage Gap	Average Negative Percentage Gap	Average Positive Percentage Gap	Average Negative Percentage Gap	Average Positive Percentage Gap
Low	Random	5%	-0.3	1.4	-0.2	1.0	-0.3	1.0
		10%	-0.3	4.9	-0.3	3.2	-	2.9
		15%	-	10.6	-	6.8	-	6.0
		20%	-	17.6	-	11.5	-0.1	9.9
	Systematic	5%	-0.3	0.8	-0.4	0.7	-0.5	0.7
		10%	-0.5	2.5	-0.6	1.8	-	1.8
		15%	-0.5	4.7	-0.8	3.4	-	3.5
		20%	-0.2	7.3	-0.8	5.4	-	5.6
Medium	Random	5%	-0.2	1.5	-0.2	1.2	-0.3	1.2
		10%	-	5.5	-	3.8	-0.1	3.6
		15%	-	12.1	-	8.2	-	7.4
		20%	-	20.0	-	13.7	-0.1	12
	Systematic	5%	-0.4	1.0	-0.4	0.8	-0.4	0.9
		10%	-0.6	2.7	-0.6	2.2	-	2.3
		15%	-0.5	4.9	-0.7	4.2	-	4.4
		20%	-0.1	7.0	-0.4	6.3	-	6.8
High	Random	5%	-0.2	1.7	-0.4	1.5	-0.3	1.7
		10%	-	6.2	-	5.3	-0.5	5.2
		15%	-	14.3	-	11.2	-0.9	10.3
		20%	-	23.7	-	18.4	-	16.2
	Systematic	5%	-0.4	1.0	-0.4	1.2	-0.2	1.2
		10%	-0.6	2.6	-0.6	2.9	-	3.3
		15%	-0.1	4.9	-0.4	5.2	-	6.0
		20%	-	6.7	-0.3	7.5	-	9.1

Figure 11a reveals that for the shortest replenishment cycles, systematically moving 5% of supply provide more runs with “better than optimal” performance. However, that altered allocation only performs 0.4% better than the optimal allocation, whereas the optimal allocation outperforms that altered solution by up to 1%. Table 9 reports the averaged percent of positive and negative gaps of altered allocations with respect to the optimal allocation. Without exception, the average positive percentage gap exceeds the average positive percentage gap.

In light of these percentages, it can clearly be observed that our optimal allocation is superior across all three distributions. Even where there is a greater tendency for optimal allocation to be inferior, the percentages indicate that optimal allocations outperform altered allocations across every subset of parameter values.

## References

- Ahani, N., T. Andersson, A. Martinello, A. Teytelboym, A. C. Trapp. 2021. Placement optimization in refugee resettlement. *Forthcoming, Operations Research*. URL [https://ideas.repec.org/p/hhs/lunewp/2018\\_023.html](https://ideas.repec.org/p/hhs/lunewp/2018_023.html).
- Al-Rousan, T., Z. Schwabkey, L. Jirmanus, B. D. Nelson. 2018. Health needs and priorities of Syrian refugees in camps and urban settings in Jordan: Perspectives of refugees and health care providers. *Eastern Mediterranean Health Journal* **24**(3) 243–253.
- Altay, N., A. Narayanan. 2020. Forecasting in humanitarian operations: Literature review and research needs. *International Journal of Forecasting* .
- Balcik, B., B. M. Beamon. 2008. Facility location in humanitarian relief. *International Journal of Logistics Research and Applications* **11**(2) 101–121.
- Balcik, B., B. M. Beamon, C. C. Krejci, K. M. Muramatsu, M. Ramirez. 2010. Coordination in humanitarian relief chains: Practices, challenges and opportunities. *International Journal of production economics* **126**(1) 22–34.
- Balcik, B., C. D. C. Bozkir, O. E. Kundakcioglu. 2016. A literature review on inventory management in humanitarian supply chains. *Surveys in Operations Research and Management Science* **21**(2) 101–116.
- Bansak, K., J. Ferwerda, J. Hainmueller, A. Dillon, D. Hangartner, D. Lawrence, J. Weinstein. 2018. Improving refugee integration through data-driven algorithmic assignment. *Science* **359**(6373) 325–329.
- Bazaraa, M. S., H. D. Sherali, C. M. Shetty. 2013. *Nonlinear programming: Theory and algorithms*. John Wiley & Sons.
- Beamon, B. M., S. A. Kotleba. 2006a. Inventory management support systems for emergency humanitarian relief operations in South Sudan. *The International Journal of Logistics Management* **17** 187–212.
- Beamon, B. M., S. A. Kotleba. 2006b. Inventory modelling for complex emergencies in humanitarian relief operations. *International Journal of Logistics Research and Applications* **9**(1) 1–18.
- Brookland, J. 2012. In USAID procurement, a game of stop-and-go. *DEVEX* URL <https://www.devex.com/news/in-usaid-procurement-a-game-of-stop-and-go-79023>. Accessed: 2020-11-04.
- Buluç, E. N. 2018. Covering vehicle routing problem: Applications for refugee related services. Master’s thesis, Bilkent University.
- COIN-OR. 2020. CBC user guide. URL <http://www.coin-or.org/cbc>.
- Crea, T. M., R. Calvo, M. Loughry. 2015. Refugee health and wellbeing: Differences between urban and camp-based environments in Sub-Saharan Africa. *Journal of Refugee Studies* **28**(3) 319–330.
- Doraï, M. K. 2010. *Manifestations of Identity: The Lived Reality of Palestinian Refugees in Lebanon*, chap. From camp dwellers to urban refugees? Urbanization and marginalization of refugee camps in Lebanon. 75–92.

- Dunn, E. C. 2016. Refugee protection and resettlement problems. *Science* **352**(6287) 772–773.
- Duran, S., M. A. Gutierrez, P. Keskinocak. 2011. Pre-positioning of emergency items for care international. *Interfaces* **41**(3) 223–237.
- Ekmekci, P. E. 2016. Syrian refugees, health and migration legislation in Turkey. *Journal of Immigrant Minority Health* URL <https://link.springer.com/content/pdf/10.1007/s10903-016-0405-3.pdf>.
- Fallon, K. 2020. Lesbos coronavirus case sparks fears for refugee camp. *The Guardian* URL <https://www.theguardian.com/global-development/2020/mar/11/lesbos-coronavirus-case-sparks-fears-for-refugee-camp-moria>. Accessed: 2020-11-04.
- Green, L. 2006. Queueing analysis in healthcare. R. W. Hall, ed., *Patient Flow: Reducing Delay in Healthcare Delivery*. Springer US, Boston, MA, 281–307. URL [https://doi.org/10.1007/978-0-387-33636-7\\_10](https://doi.org/10.1007/978-0-387-33636-7_10).
- Green, L. V., J. Soares, J. F. Giglio, R. A. Green. 2006. Using queueing theory to increase the effectiveness of emergency department provider staffing. *Academic Emergency Medicine* **13**(1) 61–68.
- Gurobi. 2020. *Gurobi Optimizer 8.0.4 Reference Manual*. Gurobi Optimization, Inc.
- Gutjahr, W. J., S. Fischer. 2018. Equity and deprivation costs in humanitarian logistics. *European Journal of Operational Research* **270**(1) 185–197.
- Holguín-Veras, J., J. Amaya-Leal, V. Cantillo, L. N. Van Wassenhove, F. Aros-Vera, M. Jaller. 2016. Econometric estimation of deprivation cost functions: A contingent valuation experiment. *Journal of Operations Management* **45** 44–56.
- Holguín-Veras, J., N. Pérez, M. Jaller, L. N. Van Wassenhove, F. Aros-Vera. 2013. On the appropriate objective function for post-disaster humanitarian logistics models. *Journal of Operations Management* **31**(5) 262–280.
- Howayek, C. 2015. No place like a refugee camp: An urban approach to refugee camps – A case study of Al Zaatari Syrian refugee camp in Jordan. Ph.D. thesis.
- IBM. 2020. IBM ILOG CPLEX 12.9 User’s Manual.
- IOM. 2019. World Migration Report 2020. Tech. rep., International Organization for Migration, Geneva, Switzerland. URL [https://www.un.org/sites/un2.un.org/files/wmr\\_2020.pdf](https://www.un.org/sites/un2.un.org/files/wmr_2020.pdf).
- IOM, NRC, and UNHCR. 2015. Camp management toolkit. Tech. rep., International Organization for Migration, Norwegian Refugee Council, United Nations High Commissioner for Refugees. URL <https://www.refworld.org/pdfid/526f6cde4.pdf>.
- Jahre, M., J. Kembro, A. Adjahossou, N. Altay. 2018. Approaches to the design of refugee camps: An empirical study in Kenya, Ethiopia, Greece, and Turkey. *Journal of Humanitarian Logistics and Supply Chain Management* **8**(3) 323–345.
- Jahre, M., J. Kembro, T. Rezvanian, O. Ergun, S. J. Håpnes, P. Berling. 2016. Integrating supply chains for emergencies and ongoing operations in UNHCR. *Journal of Operations Management* **45** 57–72.

- Karsu, O., B. Y. Kara, B. Selvi. 2019. The refugee camp management: A general framework and a unifying decision-making model. *Journal of Humanitarian Logistics and Supply Chain Management* **9** 131–150.
- Kim, S.-C., I. Horowitz, K. K. Young, T. A. Buckley. 1999. Analysis of capacity management of the intensive care unit in a hospital. *European Journal of Operational Research* **115**(1) 36–46.
- Lam, E., A. McCarthy, M. Brennan. 2015. Vaccine-preventable diseases in humanitarian emergencies among refugee and internally-displaced populations. *Human Vaccines & Immunotherapeutics* **11**(11) 2627–2636.
- Landau, L. B. 2014. Urban refugees and IDPs. *The Oxford Handbook of refugee and forced migration studies* 139–150.
- McCoy, J. H., M. L. Brandeau. 2011. Efficient stockpiling and shipping policies for humanitarian relief: UNHCR’s inventory challenge. *OR Spectrum* **33**(3) 673–698.
- Mete, H. O., Z. B. Zabinsky. 2010. Stochastic optimization of medical supply location and distribution in disaster management. *International Journal of Production Economics* **126**(1) 76–84.
- Ministry Interior of Turkey. 2020. Directorate General of Migration Management – Temporary protection. URL <https://en.goc.gov.tr/temporary-protection27>. Accessed: 2020-11-04.
- Mitchell, S., M. O’Sullivan, I. Dunning. 2020. PuLP: A linear programming toolkit for Python. URL <https://github.com/coin-or/pulp>.
- Mizushima, M., J. Coyne, S. De Leeuw, L. Kopczak, J. McCoy. 2008. Assuring effective supply chain management to support UNHCR’s beneficiaries: An independent evaluation commissioned by the policy development and evaluation service. Tech. rep. URL <https://www.unhcr.org/en-us/research/evalreports/496db70a4/assuring-effective-supply-chain-management-support-unhcrs-beneficiaries.html>.
- Natarajan, K. V., J. M. Swaminathan. 2014. Inventory management in humanitarian operations: Impact of amount, schedule, and uncertainty in funding. *Manufacturing & Service Operations Management* **16**(4) 595–603.
- Natarajan, K. V., J. M. Swaminathan. 2017. Multi-treatment inventory allocation in humanitarian health settings under funding constraints. *Production and Operations Management* **26**(6) 1015–1034.
- Rawls, C. G., M. A. Turnquist. 2010. Pre-positioning of emergency supplies for disaster response. *Transportation Research Part B: Methodological* **44**(4) 521–534.
- Rennemo, S. J., K. F. Rø, L. M. Hvattum, G. Tirado. 2014. A three-stage stochastic facility routing model for disaster response planning. *Transportation Research Part E: Logistics and Transportation Review* **62** 116–135.
- Republic of Turkey Prime Ministry Disaster and Emergency Management Authority. 2014. Syrian refugees in Turkey: Field research results URL <https://www.ncbi.nlm.nih.gov/books/NBK459037/#chapter7.r1>. Accessed: 2020-11-04.
- Roni, M. S., S. D. Eksioğlu, M. Jin, S. Mamun. 2016. A hybrid inventory policy with split delivery under regular and surge demand. *International Journal of Production Economics* **172** 126–136.

- Salmerón, J., A. Apte. 2010. Stochastic optimization for natural disaster asset prepositioning. *Production and Operations Management* **19**(5) 561–574.
- Shao, J., X. Wang, C. Liang, J. Holguín-Veras. 2020. Research progress on deprivation costs in humanitarian logistics. *International Journal of Disaster Risk Reduction* **42** 1–12.
- Simmons, A. 2016. Global refugee crisis overwhelms humanitarian aid system and exacerbates its shortcomings. *Los Angeles Times* URL <https://www.latimes.com/world/global-development/la-fg-global-refugee-crisis-20160523-snap-story.html>. Accessed: 2020-11-04.
- Solomon, F. 2020. Fearing coronavirus, refugees in crowded camps have nowhere to hide. *Wall Street Journal* URL <https://www.wsj.com/articles/fearing-coronavirus-refugees-in-crowded-camps-have-nowhere-to-hide-11586251803>. Accessed: 2020-11-04.
- Swaminathan, J. 2010. Case study: Getting food to disaster victims. *Financial Times* URL <https://www.ft.com/content/edb873a2-d6ef-11df-aaab-00144feabdc0>. Accessed: 2020-11-04.
- Terefe, D. 2017. Challenges of essential medicines availability in refugee camps in Gambella, Ethiopia: The case of Jawi, Tierikidi and Nguyiel. Ph.D. thesis, Addis Ababa University.
- Torun, P., M. M. Karaaslan, B. Sandıklı, C. Acar, E. Shurtleff, S. Dhrolia, B. Herek. 2018. Health and health care access for Syrian refugees living in Istanbul. *International Journal of Public Health* **63**(5) 601–608.
- Trapp, A. C. 2021. Source code for refugee aid allocation under uncertainty. <http://users.wpi.edu/~atrapp/tools-and-software.htm>.
- Tumen, S. 2016. The economic impact of Syrian refugees on host countries: Quasi-experimental evidence from Turkey. *The American Economic Review* **106**(5) 456–460.
- Turkish Refugee Association. 2020. Statistics about refugee population in Turkey as of 2020 URL <https://multeciler.org.tr/turkiyedeki-suriyeli-sayisi>. Accessed: 2020-11-04.
- UNHCR. 2009. The Office of the United Nations High Commissioner for Refugees (UNHCR) Global Trends – Forced Displacement in 2008. <https://www.unhcr.org/en-us/statistics/country/4a375c426/2008-global-trends-refugees-asylum-seekers-returnees-internally-displaced.html>. Accessed: 2020-11-04.
- UNHCR. 2014. Policy on alternatives to camps. URL <https://www.unhcr.org/protection/statelessness/5422b8f09/unhcr-policy-alternatives-camps.html>.
- UNHCR. 2015. High Commissioner Guterres’ Press Conference Transcript. [https://s3.amazonaws.com/unhcrsharedmedia/2015-06-18-global-trends/Video+/2015\\_06\\_18+\\_turkey\\_high\\_commissioner\\_global\\_trends\\_presser.docx](https://s3.amazonaws.com/unhcrsharedmedia/2015-06-18-global-trends/Video+/2015_06_18+_turkey_high_commissioner_global_trends_presser.docx). Accessed: 2020-11-04.
- UNHCR. 2016. Global Resettlement Needs 2017. URL <https://www.unhcr.org/en-us/protection/resettlement/575836267/unhcr-projected-global-resettlement-needs-2017.html?query=global%20resettlement%20needs%202017>.

- UNHCR. 2018. Global Trends: Forced Displacement in 2017. Tech. rep., United Nations High Commissioner for Refugees. URL <https://www.unhcr.org/globaltrends2017>.
- UNHCR. 2019. The Office of the United Nations High Commissioner for Refugees (UNHCR) Global Trends – Forced Displacement in 2018. <http://www.unhcr.org/globaltrends2018>. Accessed: 2020-11-04.
- UNHCR. 2020. Document – UNHCR Turkey: Syrian refugee camps and provincial breakdown of Syrian refugees registered in South East Turkey – March 2020. URL <https://data2.unhcr.org/en/documents/details/74445>. Accessed: 2020-11-04.
- UNICEF. 2007. *Programme Policy and Procedures Manual: Programme Operations*. URL <https://www.alnap.org/help-library/programme-policy-and-procedure-manual-programme-operations-revised-february-2007>.
- Vatasoiu, S., M. Carlsen, J. Romanski. 2015. Optimizing the size and location of short-term refugee camps in Syria. Tech. rep. URL [http://www.dam.brown.edu/people/ciocanel/Syrian\\_Refugee\\_Camps.pdf](http://www.dam.brown.edu/people/ciocanel/Syrian_Refugee_Camps.pdf).
- Vielma, J. P., S. Ahmed, G. Nemhauser. 2010. Mixed-integer models for nonseparable piecewise-linear optimization: Unifying framework and extensions. *Operations Research* **58**(2) 303–315.